Electronic Supplementary Information

Structural and computational study of reversibly photo switchable (*E*)-4-((4-alkoxyphenyl)diazenyl)benzonitrile based liquid crystals

Jyoti Swarup Thakur,[1] Omkar Dash,[1] Nagesh A. Bhale,[2] Pradip Kumar Mondal,[3] Amol G. Dikundwar,[2] Maurizio Polentarutti[3] and Susanta K. Nayak[1]*

[1]Department of Chemistry, Visvesvaraya National Institute of Technology (VNIT), Nagpur, Maharashtra-440010, India.

[2]Department of Pharmaceutical Analysis, National Institute of Pharmaceutical Education and Research (NIPER) Hyderabad, Balanagar, Hyderabad 500037, India.

[3]Elettra-Sincrotrone Trieste, S.C.p.A., S. S. 14, Km 163.5 in Area Science Park, Basovizza 34149, Italy.

Table of Contents

1. Experimental and Computational Details

1.1. Materials

The synthesis grade chemicals, 4-aminobenzonitrile and 1-bromoalkanes, were purchased from Sigma Aldrich. Phenol and reagents such as NaOH, HCl, K_2CO_3, and KI were from Fischer Scientific. They were used without further purification. The solvents were acquired from Finar and distilled, whenever required using standard procedures.

1.2. Measurements

1.2.1. Fourier-Transform Infrared Spectroscopy (FTIR)

The compounds, **AZN** and **AZN-n** were characterized by Shimadzu FT-IR (IRAFFINITY-1 CE) spectrophotometer, equipped with a (DTGS) detector and a Ge/KBr beam splitter, utilizing DRS 8000 setup using dried FTIR grade KBr (sigma). The data was collected under the ambient conditions in the range of 4000 to 400 cm^{-1} with 40 scans at a 4 cm^{-1} resolution using IR solution software.

1.2.2. NMR Spectroscopy

The synthesized compounds were identified and their purity were analyzed by NMR spectroscopy using a Bruker (400/500MHz) NMR spectrometer, Bruker, Germany using tetramethylsilane as internal standard. The NMR (^1H and ^{13}C) data for the compounds, **AZN** and **AZN-n** were collected in deuterated DMSO and chloroform, respectively. MestReNova software was utilized to analyze the data and export the graphics.

1.2.3. Crystal Growth Methods and Single crystal X-ray diffraction (SCXRD) studies

10 mg of each compound, **AZN-n** (**n = 3 - 12**) were taken in a 5 ml glass vial and dissolved in different solvents. The vials were covered with paraffin film with a pinhole and the solvent was allowed to evaporate at room temperature in a vibration free and dust free environment. The good quality plate shaped crystals suitable for X-ray diffraction were obtained only for the compounds, **AZN-n** (**n = 3**, **6**, **7**, **9**, **10** and **11**) in ethyl acetate solvent (**Fig. S5**).

The structural aspects for the obtained single crystals were analyzed by single crystal X-ray diffraction study utilizing the X-ray diffraction beamline (XRD1) at the Elettra Synchrotron facility (Trieste, Italy).[1] The crystals were dipped in NHV oil (Jena Bioscience, Germany) and then placed in a nylon loop (MiTeGen, Ithaca, USA), followed by their attachment to the goniometer head. The X-ray diffraction experiment was performed by maintaining the wavelength of the beam at 0.7 Å. The temperature was set at 100K using Oxford Cryo Stream 700. The diffraction data was indexed and integrated by XDS software[2] and the absorption correction was performed using SADABS.[3] The Olex-2-1.5[4] package, employing the Intrinsic phasing ShelXT program was utilized for the structure solution and refinement was carried out with ShelXL package[5] through least squares minimization. All the non-hydrogen atoms were refined anisotropically and the hydrogen atoms were fixed in the diffraction maps with the C-H bond distances fixed at 0.95 Å for CH, 0.99 Å for CH2, and 0.98 Å for CH3. The molecular packings in these compounds were illustrated by using Mercury 4.2.0 program.[6]

1.2.4. Powder X-ray diffraction (PXRD) studies

Bruker D8 Advance Eco X-ray diffractometer with Ni, filtered CuK_{α}= 1.54056 Å radiation and Lynxeye detector was utilized to collect the PXRD data. The data was collected at room temperature using a zero background Si sample holder. The dispersed intensities were recorded using a scintillation counter. The angular range (2θ) was set 5 to 60º with a step size of 0.02º along

with 0.3 seconds per step measuring time. Diffract. Eva software suit was utilized to analyze the data.

1.2.5. Differential Scanning Calorimetry (DSC)

Differential Scanning Calorimetry (DSC) analysis was carried out utilizing Discovery Series DSC 2500, TA Instruments, New Castle, Delaware, USA with heating as well as cooling at a rate of 10 ^{o} C min^{-1} under nitrogen atmosphere (flow rate = 50 mL/min). The second heating and cooling cycle was considered for the identification of the phase transitions in the compounds, **AZN-n**.

1.2.6. Hot stage Polarized Optical Microscopy (POM)

The microscopic textures of the liquid crystalline (LC) phases were visualized using Nikon Polarized optical microscope equipped with a Linkam LTS 420 hot stage with heating and cooling rate of 5˚C /min. The measurements were carried out by sandwiching the solid sample between a glass slide and a cover slip. The photoresponsive nature in LC state for the samples were carried out using a UV light (1 W) source of 365 nm.

1.2.7. UV-Visible (UV-Vis) spectroscopic studies

Photoresponsive studies were carried out in the solution state using a TestRight PRIZM Abs-UV-VIS (UV-Visible Spectrophotometer; Range: 200-1100 nm with CCD detector) by TestRight Nanosystems Pvt. Ltd., India using a 1W UV (365 nm) and Visible (510 nm) source. These studies were conducted on a μm solution of the samples in cyclohexane in a 1 cm quartz cuvette. The conversion efficiency for $E \rightarrow Z$ photoisomerization can be calculated as,

$$CE = \frac{A_o - A_\infty}{A_o}$$

Where, A_0 is the initial absorbance (before UV exposure) and A_∞ is the final absorbance (after UV exposure).

Further, the kinetics of the $E \leftrightarrow Z$ isomerization can be studied by the following equation,

$$\ln [(A_{\infty} - A_{o})/ (A_{\infty} - A_{t})] = kt$$

Where, A_0, A_t and A_∞ are the peak absorbance values at time zero, time t and time infinity, respectively and k is the rate constant.

1.3. Computational analyses

1.3.1. Hirshfeld surface (HS) analysis

Crystal Explorer 21.5 program[7] was utilized on the respective geometries obtained from SCXRD for the HS analysis.[8] Further, the percentage contributions for different interactions in the crystal packing were calculated using 2D fingerprint on the HS. Since **AZN-3** has 3 molecules in the asymmetric unit, the HS calculations were carried out for each unique molecule.

1.3.2. Energy framework (EF) analysis

The quantitative description of the 3D-topology of the weak inter molecular interactions in the crystal packing with the partitioned energies between the molecular pairs can be described by the energy framework (EF) analysis.[9] The calculations were carried out in the *Crystal Explorer 21.5* software at the B3LYP/6-31G (d, p) level using the default Tonto program for **AZN-n** (**n = 3**, **6**, **7**, **9**, **10** and **11**). The 3D cluster was generated around the selected asymmetric unit within a radius of 3.8 Å. Similar to the HS surface for each unique molecule in **AZN-3**, the cluster was generated. The interaction energies were represented by the cylinders connecting the center of the molecular pairs. The radii of the cylinders are proportional to the strength of these interactions, with the tube size fixed at 100 and the cut-off value set at 0 kJ/mol. The various components, such as total interaction, dispersion, and electrostatic energies, are illustrated by the blue, green and red color cylinders, respectively.

1.3.3. Density functional theory (DFT) analysis

The single point energy calculations for the compounds, **AZN-n** (**n = 3**, **6**, **7**, **9**, **10** and **11**) were carried out by Density Functional Theory (DFT) utilizing the Gaussian 09 program.[10] The Becke, 3-parameter, Lee-Yang-Parr (B3LYP) level of theory with 6311-G (d, p) basis set was utilized. The results were visualized using the Gauss View visualization software.[11] Further, the qualitative and quantitative analysis of HBs and Cg···Cg (π···π) as well as C-H···π interactions was carried out by the non-covalent interactions index (NCI) and quantum theory of atoms in molecules (QTAIM) investigations using Multiwfn 3.8 software.[12] The charge transfer interaction between N/O and the H atoms involved in HBs were revealed by the Natural bond orbital (NBO) analysis using NBO 6.0 program.[13] The Visual Molecular Dynamics (VMD) program[14] was utilized to visualize these results. All these calculations were carried out by taking the major disorder component in **AZN-3**.

The characterization of synthesized (*E*)-4-((4-hydroxyphenyl)diazenyl)benzonitrile (**AZN**) and its alkoxy derivatives (**AZN-n**) as per **Scheme 1** were provided as follows:

1.4. Synthesis

1.4.1. Synthesis of (*E*)-4-((4-hydroxyphenyl)diazenyl)benzonitrile (AZN)

An aqueous solution of sodium nitrite (0.035 moles) was gradually added to a solution containing 4-aminobenzonitrile (0.035 moles) and hydrochloric acid (11.3 N, 8 mL) in 20 mL water at 0-5 °C and stirred for 1 hour, forming a diazonium salt. The formed diazonium salt was then added dropwise to an aqueous solution containing phenol (0.0355 moles) and 22.5 ml of sodium hydroxide (10% w/v), which was maintained at 0-5 °C, followed by stirring for 3 hours. The reaction mixture was then acidified to pH 6 to yield an orange colored precipitate. The crude product was then filtered and washed several times with distilled water, followed by drying in a vacuum oven at 90 °C for 24 hours.[15] The product was confirmed by FTIR, NMR (^{1}H and ^{13}C) spectroscopic techniques (**Fig. S1** and **S2**).

Yield: 92%

FT-IR (KBr, cm^{-1}): 3329 (O-H), 2239 (CN), 1607, 1587 (C=C, aromatic).

^{1}H NMR (500 MHz, DMSO-d_6, ppm), δ: 10.58 (s, 1H), 8.02 (d, J = 8.4 Hz, 2H), 7.92 (d, J = 8.5 Hz, 2H), 7.85 (d, J = 8.8 Hz, 2H), 6.98 (d, J = 8.8 Hz, 2H).

^{13}C NMR (125 MHz, DMSO-d_6, ppm), δ: 162.15, 154.34, 145.28, 133.74, 125.71, 122.74, 118.59, 116.20, 112.21.

1.4.2. Synthesis of (*E*)-4-((4-alkoxyphenyl)diazenyl)benzonitrile (AZN-n)

The compound, **AZN** (1 equivalent, 2.2397 mmoles), K_2CO_3 (2 equivalents, 4.4794 mmoles), and catalytic amount of KI in butanone (20 ml) were taken in a round bottom (RB) flask and refluxed for 15 minutes. The corresponding 1-bromoalkane (1.1 equivalents, 2.4637 mmoles) was added to the reaction mixture and refluxed for 16 hours. The completion of the reaction was monitored by thin-layer chromatography (TLC) using ethyl acetate: petroleum ether (60-80) as the mobile phase. The reaction mixture was filtered and the solvent was evaporated by the rotary evaporator. The crude product was purified by silica gel column chromatography using ethyl acetate: pet ether (60-80) solvent system (1:9) having 72-78 % yield, which was further characterized by FTIR, NMR (^{1}H and ^{13}C) spectroscopic techniques (**Fig. S1** and **S2-S4**).

1.4.3. Characterization by FTIR and NMR spectroscopy

AZN-3: Orange powder (74% yield)

FTIR (KBr cm^{-1}): 3044 (CH_3), 2968, 2878 (CH_2), 2222 (CN), 1602, 1579 (C=C, aromatic), 1248 (C_{ar}-O-C), 1136 (O-C-C).

^{1}H NMR (400 MHz, Chloroform-*d*, ppm) δ: 7.94 (d, J = 9.0 Hz, 4H), 7.79 (d, J = 8.7 Hz, 2H), 7.02 (d, J = 9.0 Hz, 2H), 4.02 (t, J = 6.6 Hz, 2H), 1.85 (m, 2H), 1.07 (t, J = 7.4 Hz, 3H).

^{13}C NMR (101 MHz, Chloroform-*d*, ppm) δ: 163.22, 155.23, 147.11, 133.62, 125.94, 123.52, 119.16, 115.33, 113.55, 70.40, 22.94, 10.95.

AZN-4: Orange powder (77% yield)

FTIR (KBr cm^{-1}): 3045 (CH_3), 2960, 2872 (CH_2), 2222 (CN), 1602, 1579 (C=C, aromatic), 1252 (C_{ar}-O-C), 1142 (O-C-C).

^{1}H NMR (400 MHz, Chloroform-*d*, ppm) δ: 7.94 (d, J = 6.9 Hz, 4H), 7.78 (d, J = 8.5 Hz, 2H), 7.02 (d, J = 9.0 Hz, 2H), 4.07 (t, J = 6.5 Hz, 2H), 1.82 (m, 2H), 1.53 (m, 2H), 1.00 (t, J = 7.4 Hz, 3H).

^{13}C NMR (101 MHz, Chloroform-*d*, ppm) δ: 162.95, 146.86, 133.30, 125.62, 123.21, 118.81, 115.04, 113.28, 31.33, 19.35, 13.96.

AZN-5: Orange powder (75% yield)

FTIR (KBr cm^{-1}): 3045 (CH_3), 2959, 2872 (CH_2), 2222.7 (CN), 1602, 1583 (C=C, aromatic), 1252 (C_{ar}-O-C),1142 (O-C-C).

^{1}H NMR (400 MHz, Chloroform-*d*, ppm) δ: 7.94 (d, *J* = 6.9 Hz, 4H), 7.78 (d, *J* = 8.4 Hz, 2H), 7.02 (d, *J* = 9.0 Hz, 2H), 4.06 (t, *J* = 6.6 Hz, 2H), 1.84 (m, 2H), 1.42 (m, 4H), 0.95 (t, *J* = 7.1 Hz, 3H).

^{13}C NMR (101 MHz, Chloroform-*d*, ppm) δ: 162.94, 154.97, 146.85, 133.30, 125.62, 118.81, 113.28, 68.65, 28.98, 28.29, 22.58, 14.15.

AZN-6: Orange powder (73% yield)

FTIR (KBr cm^{-1}): 3046 (CH_3), 2952, 2865 (CH_2), 2221.5 (CN), 1602, 1583 (C=C, aromatic), 1252 (C_{ar}-O-C), 1139 (O-C-C).

^{1}H NMR (500 MHz, Chloroform-*d*, ppm) δ: 7.93 (d, *J* = 10.9 Hz, 4H), 7.78 (d, *J* = 8.7 Hz, 2H), 7.02 (d, *J* = 9.0 Hz, 2H), 4.06 (t, *J* = 6.6 Hz, 2H), 1.83 (m, 2H), 1.48 (m, 2H), 1.36 (m, 4H), 0.95 (t, *J* = 7.4 Hz, 3H).

^{13}C NMR (126 MHz, Chloroform-*d*, ppm) δ: 162.92, 154.97, 146.83, 133.30, 125.61, 123.21, 118.82, 115.03, 113.25, 68.65, 31.69, 29.25, 25.81, 14.17.

AZN-7: Orange powder (75% yield)

FTIR (KBr cm^{-1}): 3046 (CH_3), 2955, 2849 (CH_2), 2221 (CN), 1600, 1581 (C=C, aromatic), 1249 (C_{ar}-O-C), 1139 (O-C-C).

^{1}H NMR (500 MHz, Chloroform-*d*, ppm) δ: 7.93 (d, *J* = 6.9 Hz, 4H), 7.78 (d, *J* = 8.6 Hz, 2H), 7.02 (d, *J* = 9.0 Hz, 2H), 4.06 (t, *J* = 6.6 Hz, 2H), 1.85 (m, 2H), 1.48-1.36 (m, 8H), 0.90 (t, *J* = 7.4 Hz, 3H).

^{13}C NMR (126 MHz, Chloroform-*d*, ppm) δ: 162.92, 154.97, 133.30, 125.61, 123.21, 118.82, 115.03, 113.25, 68.65, 31.90, 29.29, 26.10, 22.75, 14.23.

AZN-8: Orange powder (78% yield)

FTIR (KBr cm^{-1}): 3045 (CH_3), 2952, 2869 (CH_2), 2222.7 (CN), 1602, 1583 (C=C, aromatic), 1252 (C_{ar}-O-C), 1142 (O-C-C).

^{1}H NMR (500 MHz, Chloroform-*d*, ppm) δ: 7.94 (d, *J* = 7.0 Hz, 4H), 7.79 (d, *J* = 8.6 Hz, 2H), 7.02 (d, *J* = 9.0 Hz, 2H), 4.06 (t, *J* = 6.6 Hz, 2H), 1.83 (m, 2H), 1.48 (m, 2H), 1.30 (m, 8H), 0.90 (t, *J* = 7.0 Hz, 3H).

^{13}C NMR (126 MHz, Chloroform-*d*) δ: 162.93, 154.98, 146.85, 133.30, 125.61, 123.21, 118.82, 115.04, 113.28, 68.67, 31.95, 29.37, 26.15, 22.80, 14.24.

AZN-9: Orange powder (72% yield)

FTIR (KBr cm^{-1}): 3048 (CH_3), 2948, 2852 (CH_2), 2224 (CN), 1603, 1581 (C=C, aromatic), 1256 (C_{ar}-O-C), 1136 (O-C-C).

^{1}H NMR (500 MHz, Chloroform-*d,* ppm) δ: 7.94 (d, *J* = 6.8 Hz, 4H), 7.78 (d, *J* = 8.5 Hz, 2H), 7.02 (d, *J* = 9.0 Hz, 2H), 4.06 (t, *J* = 6.5 Hz, 2H), 1.83 (m, 2H), 1.48 (m, 2H), 1.30 (m, 10H), 0.89 (t, *J* = 5.8 Hz, 3H).

^{13}C NMR (126 MHz, Chloroform-*d*, ppm) δ: 162.93, 154.98, 146.85, 133.30, 125.61, 123.21, 118.82, 115.04, 113.27, 68.66, 32.02, 29.52, 26.14, 22.81, 14.25.

AZN-10: Orange powder (70% yield)

FTIR (KBr cm^{-1}): 3045 (CH_3), 2948, 2852 (CH_2), 2221 (CN), 1601, 1582 (C=C, aromatic), 1252 (C_{ar}-O-C), 1140 (O-C-C).

^{1}H NMR (500 MHz, Chloroform-*d*, ppm) δ: 7.94 (d, *J* = 8.9 Hz, 4H), 7.78 (d, *J* = 8.5 Hz, 2H), 7.02 (d, *J* = 9.0 Hz, 2H), 4.06 (t, *J* = 6.6 Hz, 2H), 1.83 (m, 2H), 1.48-1.28 (m, 16H), 0.89 (t, *J* = 6.9 Hz, 3H).

^{13}C NMR (126 MHz, Chloroform-*d*, ppm) δ: 162.92, 154.97, 146.83, 133.30, 125.61, 123.21, 118.82, 113.26, 68.66, 32.04, 29.71, 26.14, 22.82, 14.26.

AZN-11: Orange powder (75% yield)

FTIR (KBr cm^{-1}): 3048 (CH_3), 2952, 2848 (CH_2), 2221 (CN), 1603, 1580 (C=C, aromatic), 1252 (C_{ar}-O-C), 1141 (O-C-C).

^{1}H NMR (500 MHz, Chloroform-*d*, ppm) δ: 7.94 (d, *J* = 10.5 Hz, 4H), 7.79 (d, *J* = 8.6 Hz, 2H), 7.02 (d, *J* = 9.0 Hz, 2H), 4.06 (t, *J* = 6.6 Hz, 2H), 1.83 (m, 2H), 1.48-1.27 (m, 18H), 0.88 (t, *J* = 7.0 Hz, 3H).

^{13}C NMR (126 MHz, Chloroform-*d*, ppm) δ: 162.92, 154.97, 146.84, 125.61, 123.21, 118.83, 113.26, 68.66, 32.06, 29.76, 26.14, 22.83, 14.27.

AZN-12: Orange powder (72% yield)

FTIR (KBr cm^{-1}): 3045 (CH_3), 2952, 2849 (CH_2), 2221 (CN), 1602, 1583 (C=C, aromatic), 1251 (C_{ar}-O-C), 1140 (O-C-C).

^{1}H NMR (500 MHz, Chloroform-*d*, ppm) δ: 7.94 (d, *J* = 9.1 Hz, 4H), 7.79 (d, *J* = 8.7 Hz, 2H), 4.06 (t, *J* = 6.6 Hz, 2H), 1.81 (m, 2H), 1.48 (m, 2H), 1.27 (m, 18H), 0.88 (t, *J* = 7.0 Hz, 3H).

^{13}C NMR (126 MHz, Chloroform-*d*, ppm) δ: 162.93, 154.98, 146.84, 133.31, 125.61, 123.21, 118.83, 115.04, 113.26, 68.66, 32.07, 29.51, 26.14, 22.84, 14.27.

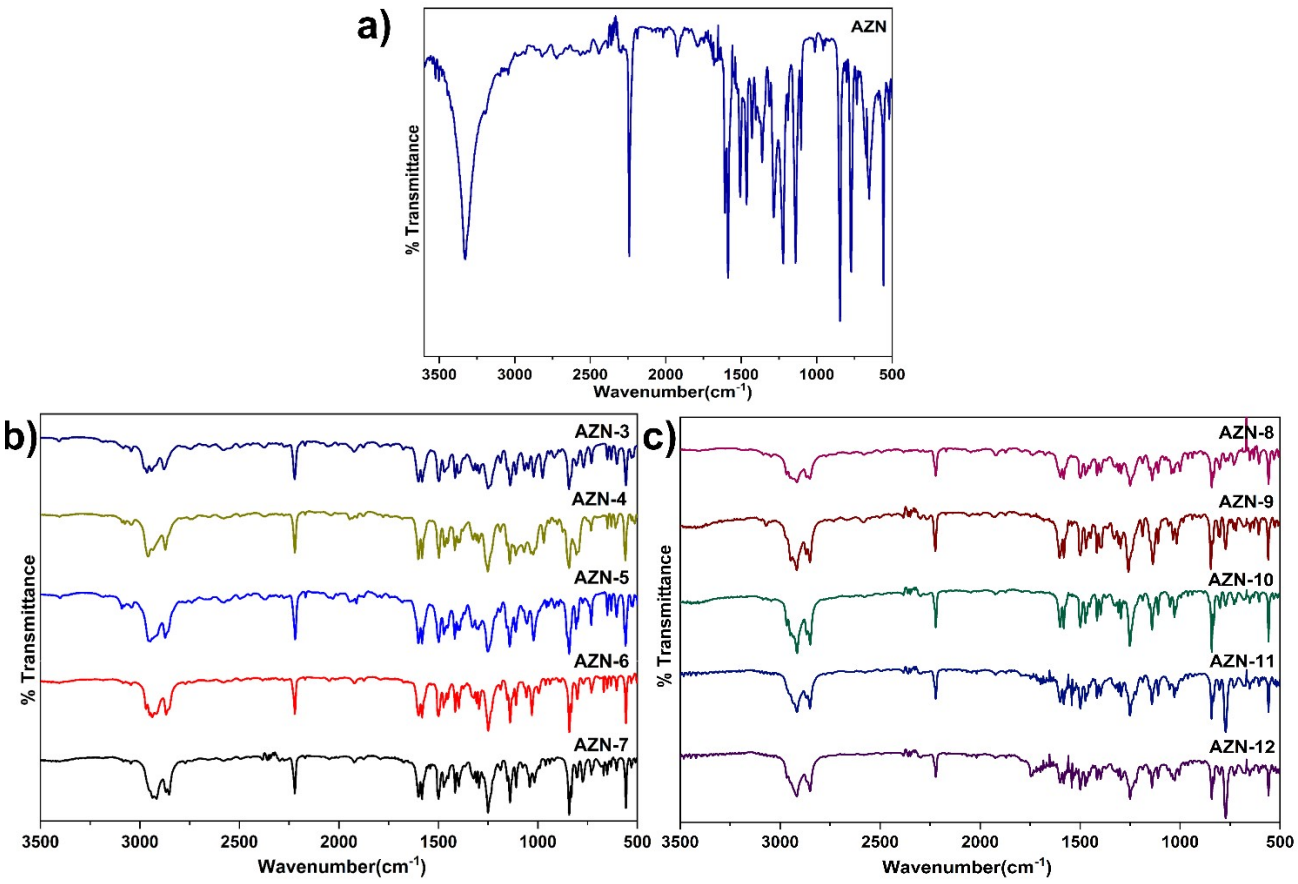

Fig. S1. FTIR spectra for a) **AZN** and b-c) **AZN-n** (**n= 3 - 12**).

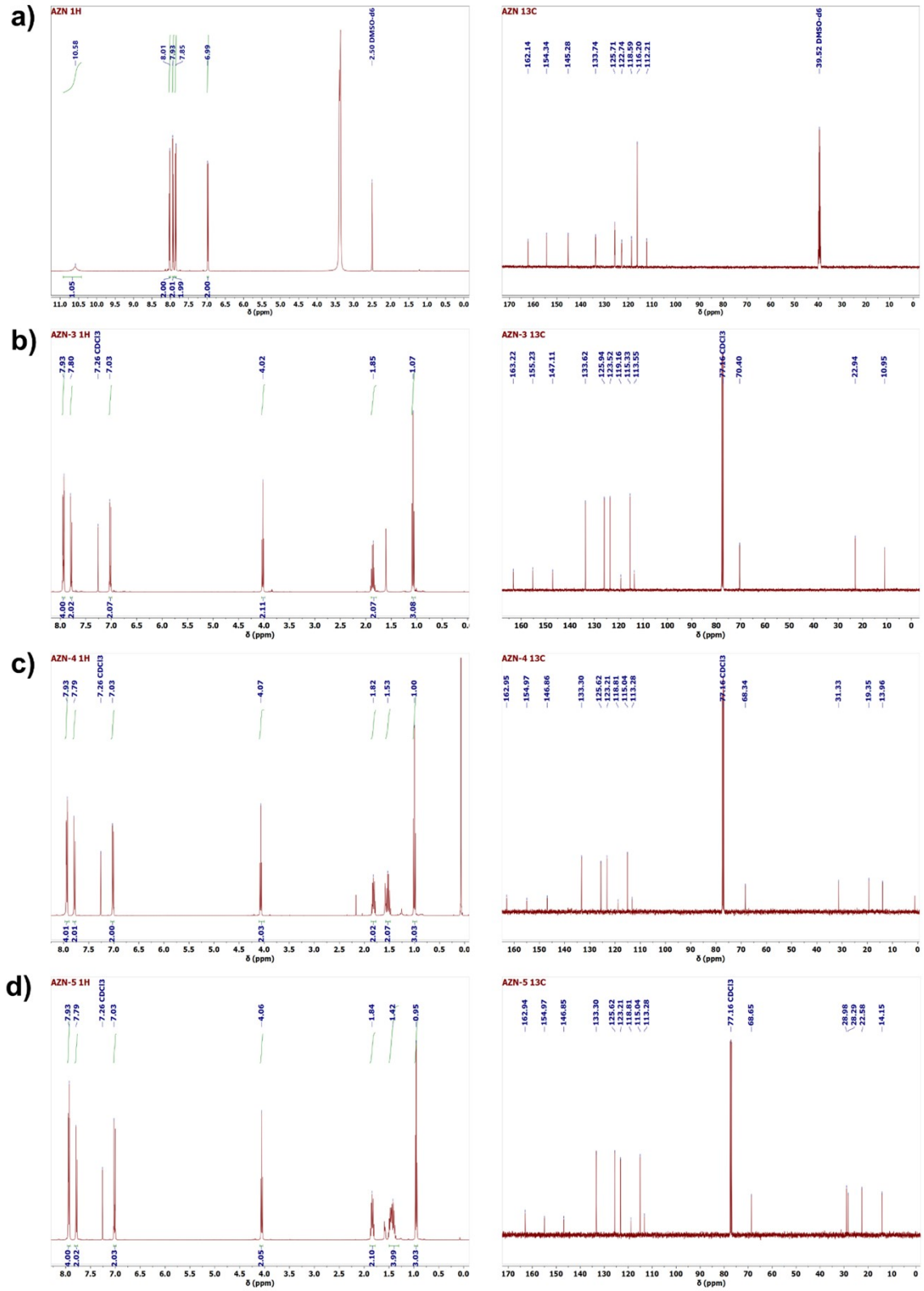

Fig. S2. ^{1}H (left) and ^{13}C (right) NMR spectra for a) **AZN**, b) **AZN-3**, c) **AZN-4** and d) **AZN-5**.

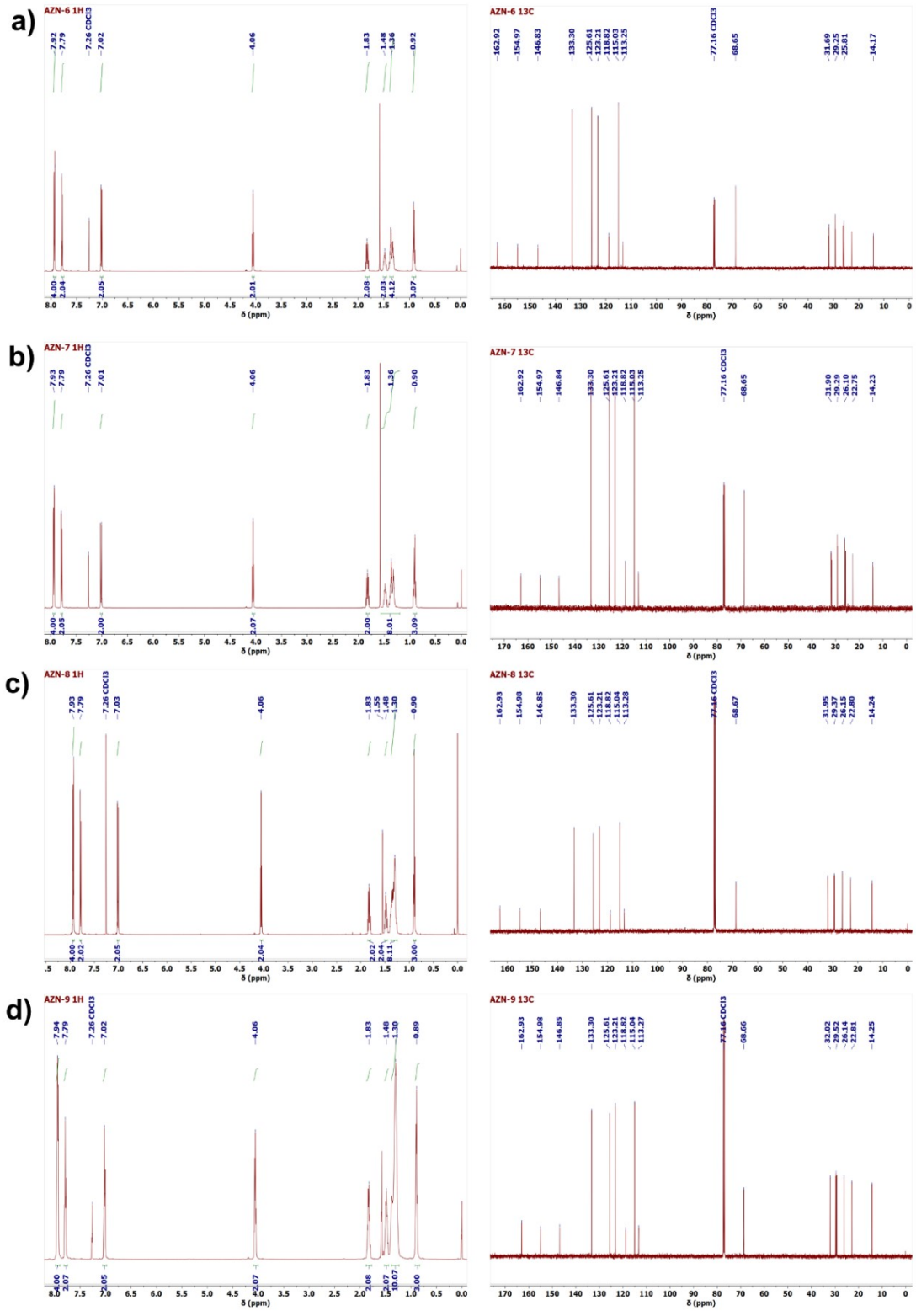

Fig. S3. ^{1}H (left) and ^{13}C (right) NMR spectra for a) **AZN-6**, b) **AZN-7**, c) **AZN-8** and d) **AZN-9**.

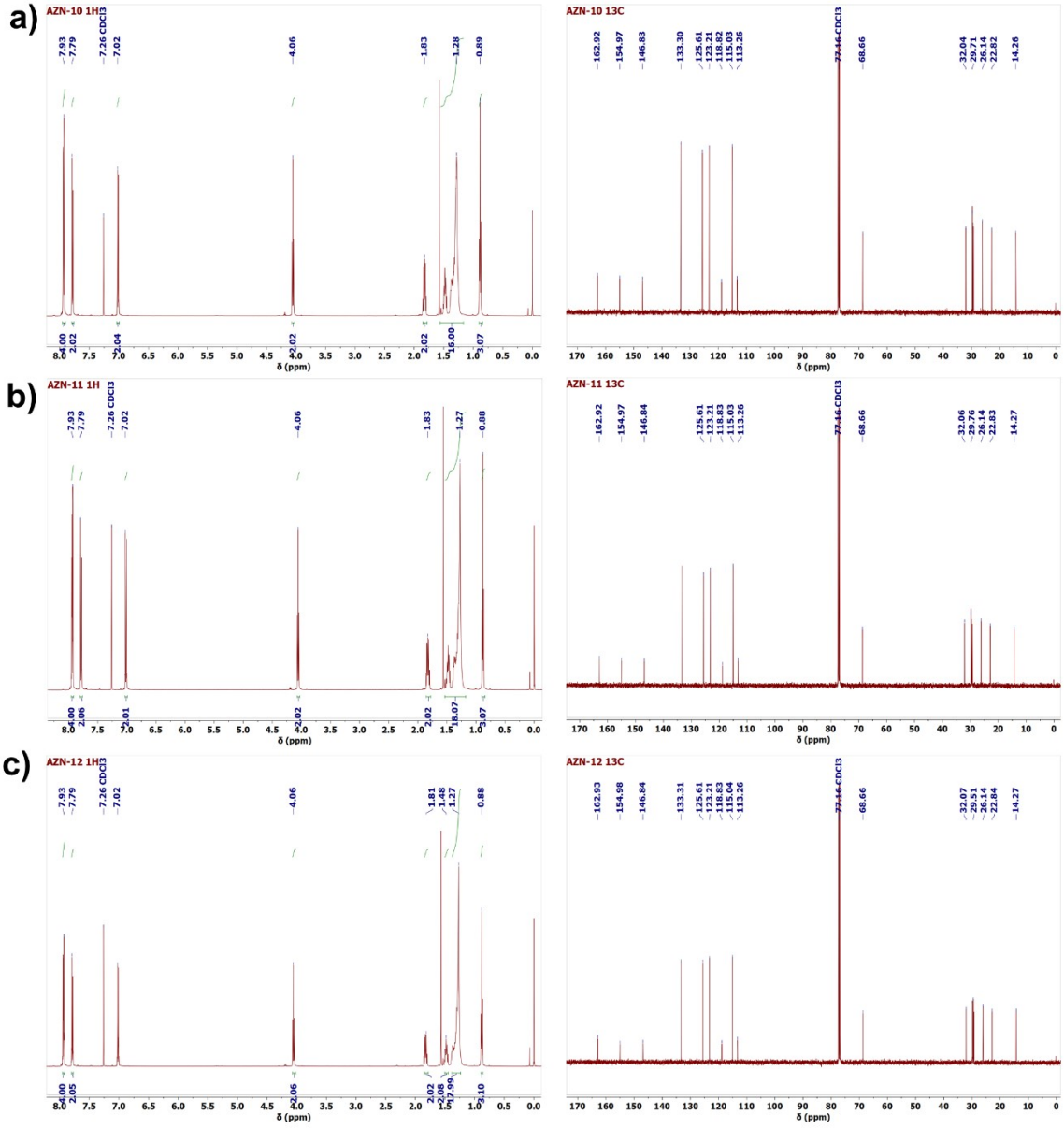

Fig. S4. ^{1}H (left) and ^{13}C (right) NMR spectra for a) **AZN-10**, b) **AZN-11** and c) **AZN-12**.

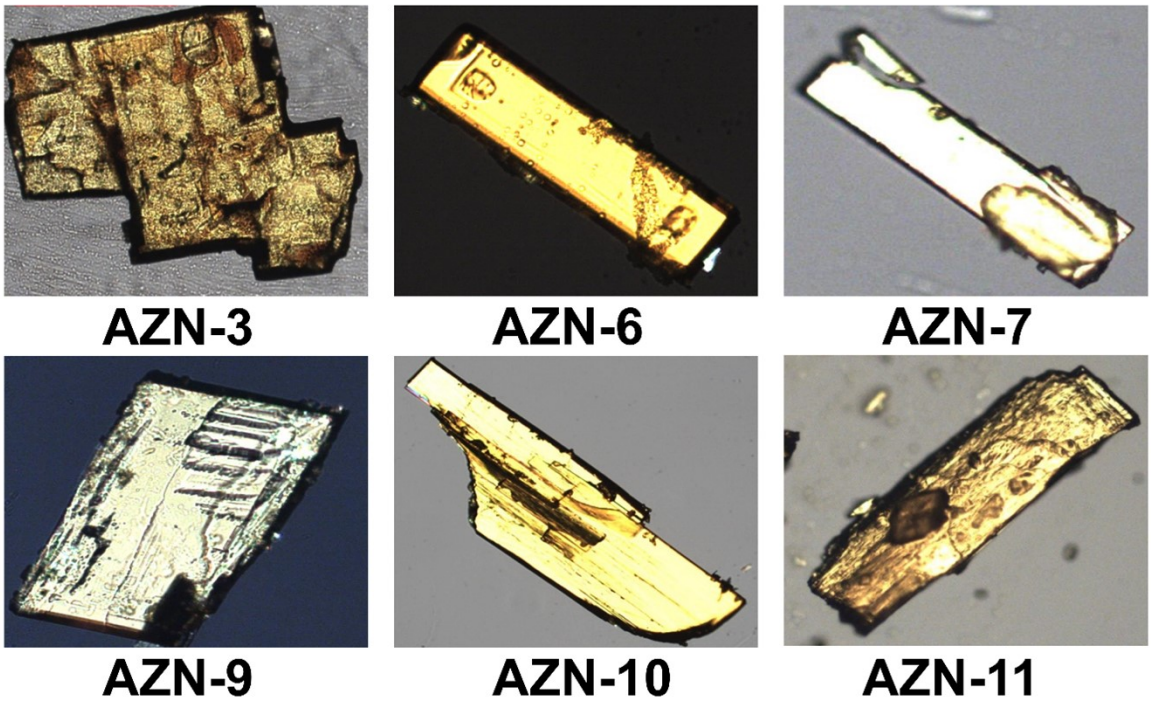

Fig. S5. Single crystal images of the compounds, **AZN-n (n= 3, 6, 7, 9, 10 and 11)**.

Table S1. Crystallographic details for the single crystals of **AZN-n** (**n= 3, 6, 7, 9, 10 and 11**).

Sample code	**AZN-3**	**AZN-6**	**AZN-7**	**AZN-9**	**AZN-10**	**AZN-11**
CCDC No.	2457153	2457151	2457152	2457150	2457154	2457155
Temperature (K)	100	100	100	100	100	100
Formula	$C_{16}H_{15}N_3O$	$C_{19}H_{21}N_3O$	$C_{20}H_{23}N_3O$	$C_{22}H_{27}N_3O$	$C_{23}H_{29}N_3O$	$C_{24}H_{31}N_3O$
a (Å)	5.9500(12)	5.8120(12)	5.8180(12)	5.8210(12)	5.7970(12)	5.8110(12)
b (Å)	18.5370(37)	7.4680(15)	7.4410(15)	11.1780(22)	7.4060(15)	7.3670(15)
c (Å)	19.1140(38)	37.4550(75)	40.7450(82)	16.2110(32)	46.4640(93)	49.5498(99)
α (°)	73.386(30)	90.000	90.000	72.803(30)	90.000	90.000
β (°)	87.851(30)	93.006(30)	92.784(30)	79.812(30)	93.229(30)	93.102(30)
γ (°)	88.909 (30)	90.000	90.000	75.362 (30)	90.000	90.000
Volume (Å^3)	2018.67(19)	1623.46(26)	1761.84(26)	968.97(12)	1991.65(34)	2118.10(35)
Formula weight	265.3	307.4	321.4	349.5	363.5	377.5
Density (g cm^{-3})	1.31	1.26	1.21	1.20	1.21	1.18
Crystal System	Triclinic	Monoclinic	Monoclinic	Triclinic	Monoclinic	Monoclinic
F(000)	840.0	656.0	688.0	376.0	784.0	816.0
Reflections collected	11765	3981	5112	4702	4856	4856
Space group	$P\bar{1}$	$P2_1/n$	$P2_1/n$	$P\bar{1}$	$P2_1/c$	$P2_1/c$
Z, Z'	6, 3	4, 1	4, 1	2, 1	4, 1	4, 1
$R_{\_all}$, $R_{\_obs}$	0.067, 0.063	0.051, 0.044	0.064, 0.058	0.058, 0.049	0.073, 0.070	0.066, 0.059
$wR_{\_all}$, $wR_{\_obs}$	0.192, 0.184	0.136, 0.135	0.170, 0.163	0.149, 0.140	0.213, 0.211	0.179, 0.172
GOOF	1.045	1.057	1.020	1.067	1.067	1.047
Δρmax, Δρmin (e$^-$ /Å^3)	0.473, -0.563	0.403, -0.355	0.540, -0.421	0.412, -0.252	0.567, -0.533	0.581, -0.518

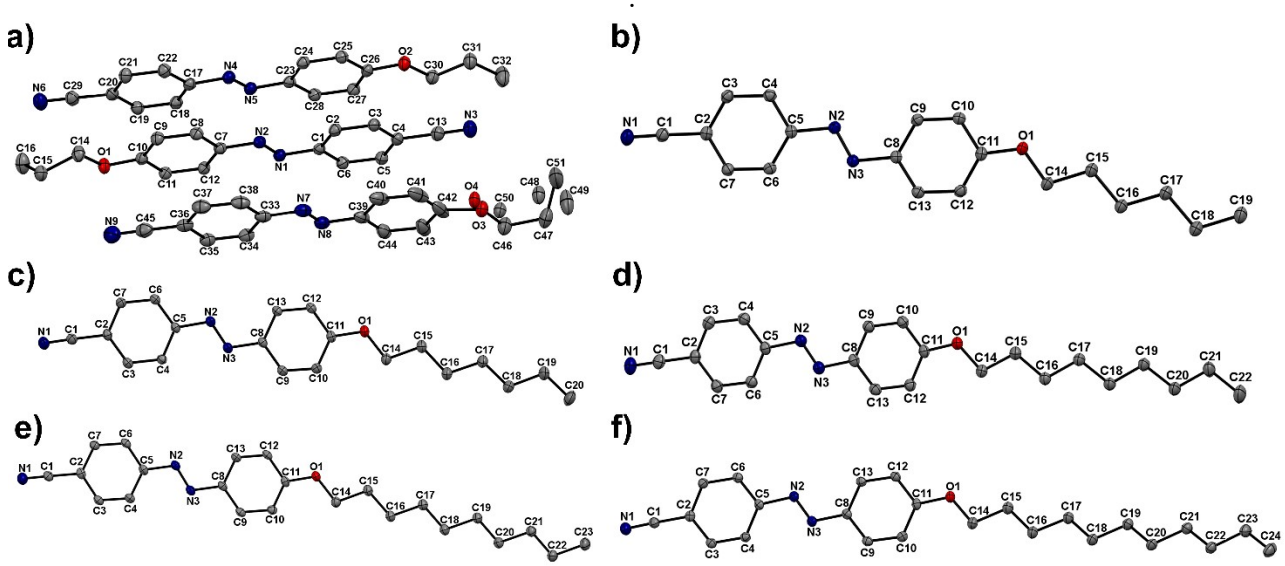

Fig. S6. ORTEP representation of molecular arrangements for a-f) **AZN-n** (**n= 3, 6, 7, 9, 10 and 11**) drawn at 50 % thermal ellipsoidal probability with atom labeling barring the hydrogen atoms.

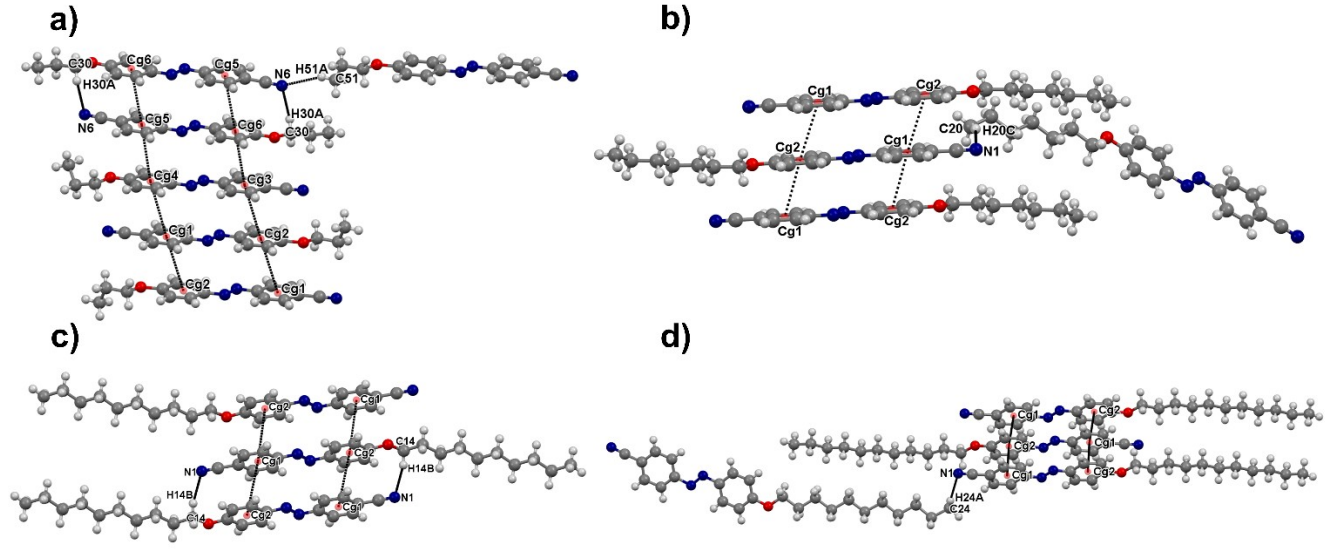

Fig. S7. Crystal packing of a) **AZN-3**, b) **AZN-7**, c) **AZN-10** and d) **AZN-11** showing the weak interactions such as C-H···N and π···π interactions.

.

Table S2. Intermolecular weak HB interactions in the crystal structure of **AZN-n (n= 3, 6, 7, 9, 10 and 11)**.

Sample code	Donor(D)-H···Acceptor	D-H (Å)	H···A (Å)	D···A (Å)	<D-H···A (°)	Symmetry code
AZN-3	C30-H30A···N6	0.99	2.72	3.395	126	1-x, 1-y, -z
	C51-H51A···N6	0.98	2.74	3.645	154	-2+x, y, 1+z
AZN-6	C14-H14B···N1	0.99	2.72	3.512	137	1-x, 1-y, -z
AZN-7	C20-H20C···N1	0.98	2.74	3.666	157	3/2+x, 3/2-y, 1/2+z
AZN-9	C10-H10···O1	0.95	2.56	3.477	146	-x, 1-y, 1-z
	C14-H14B···N1	0.99	2.68	3.452	136	2-x, -y, 1-z
AZN-10	C14-H14B···N1	0.99	2.71	3.499	137	-x, 1-y, -z
AZN-11	C24-H24A···N1	0.98	2.74	3.686	163	2+x, 3/2-y, 1/2+z

Table S3. Intermolecular weak Cg···Cg (π···π) interactions in the crystal structure of **AZN-n (n= 3, 6, 7, 9, 10 and 11)**.

Sample Code	Ring (I)-Ring(J)	*R*c(Å)[c]	α(°)[d]	b(°)[e]	γ(°)[f]	Slippage(Å)[g]	Symmetry code
AZN-3	Cg1···Cg2 [a]	3.7900(10)	0.41(5)	23.6	23.9	1.515	1-x, -y, 1-z
	Cg2···Cg3 [a]	3.7415(10)	0.45(5)	24.4	24.0	1.545	x, y, z
	Cg1···Cg4 [a]	3.8370(10)	1.45(4)	25.4	24.4	1.648	x, y, z
	Cg3···Cg6 [a]	3.6210(9)	0.70(4)	20.5	21.0	1.271	x, y, z
	Cg4···Cg5 [a]	3.7847(9)	2.57(4)	23.1	25.6	1.487	x, y, z
	Cg5···Cg6 [a]	3.7944(9)	1.11(4)	25.1	24.3	1.607	1-x, -y, -z
AZN-6	Cg1···Cg2 [b]	3.8010(8)	1.11(1)	26.8	27.1	1.716	1-x, 1-y, -z
	Cg1···Cg2 [b]	3.6715(8)	1.11(1)	24	24.1	1.491	1-x, -y, -z
AZN-7	Cg1···Cg2 [b]	3.6811(8)	0.88(2)	24.9	25.4	1.548	-x, 2-y, -z
	Cg1···Cg2 [b]	3.7623(8)	0.88(2)	25.1	25.8	1.599	-x, 1-y, -z
AZN-9	Cg1···Cg2 [b]	3.8431(8)	4.88(2)	26.2	28.2	1.700	2-x, -y, 1-z
	Cg2···Cg2 [b]	3.7683(8)	0.00(2)	23.0	23.0	1.817	1-x, 1-y, 1-z
AZN-10	Cg1···Cg2 [b]	3.7679(8)	1.03(3)	26.6	26.9	1.686	-x, 1-y, -z
	Cg1···Cg2 [b]	3.6429(8)	1.03(3)	23.8	24.0	1.468	-x, -y, -z
AZN-11	Cg1···Cg2 [b]	3.7284(8)	0.74(2)	24.8	25.4	1.564	-x, 1-y, -z
	Cg1···Cg2 [b]	3.6431(8)	0.74(2)	24,2	24.7	1.494	-x, 2-y, -z

[a]Cg1, Cg2, Cg3, Cg4, Cg5 and Cg6 are the centroids of the rings C33-C34-C35-C36-C37-C38, C39-C40-C41-C42-C43-C44, C1-C2-C3-C4-C5-C6, C7-C8-C9-C10-C11-C12, C17-C18-C19-C20-C21-C22 and C23-C24-C25-C26-C27-C28, respectively.

[b]Cg1 and Cg2 are the centroids of the rings C2-C3-C4-C5-C6-C7 and C8-C9-C10-C11-C12-C13, respectively.

[c]Centroid distance between ring I and ring J.

[d]Dihedral Angle between Planes I aand J.

[e]Angle Cg(I)-->Cg(J) or Cg(I)-->Me vector and normal to plane I.

[f]Angle Cg(I)-->Cg(J) vector and normal to plane J.

[g]Distance between Cg(I) and Perpendicular Projection of Cg(J) on Ring I

Table S4. Intermolecular weak C-H···Cg (π) interactions in the crystal structure of **AZN-9**.

Sample code	Donor(D)-H···Cg	D-H (Å)	H···Cg (Å)	D···Cg (Å)	<D-H···Cg (°)	γ	Symmetry code
AZN-9	C17-H17A···Cg1[a]	0.99	2.81	3.6712(8)	146	0.87	1-x, 1-y, 1-z

[a]Cg1 is the centroids of the ring C2-C3-C4-C5-C6-C7.

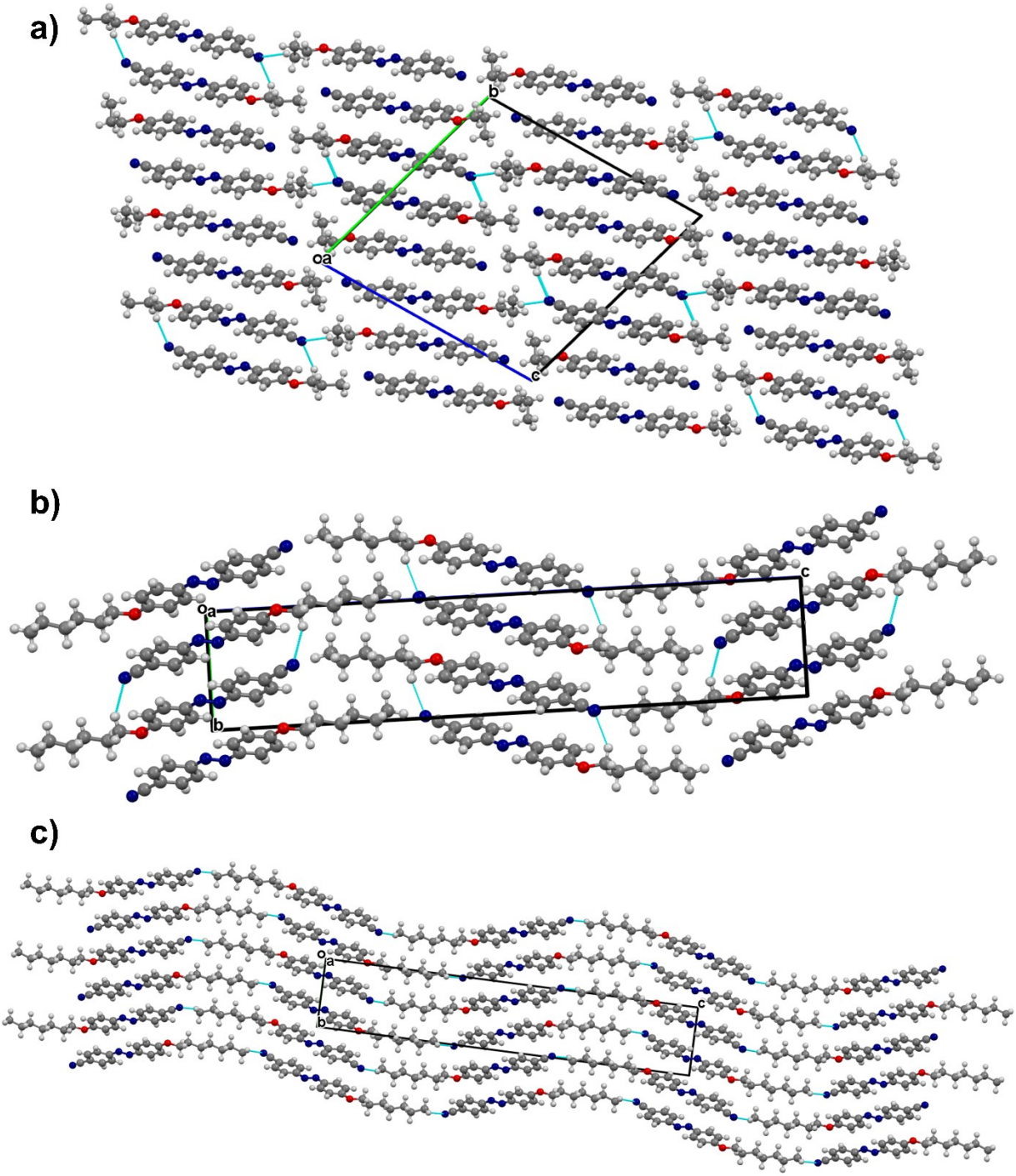

Fig. S8. Propagation of molecules in the crystal packing for a) **AZN-3**, b) **AZN-6** and c) **AZN-7** through the weak interactions such as C-H···N and π···π interactions, when viewed along a axis.

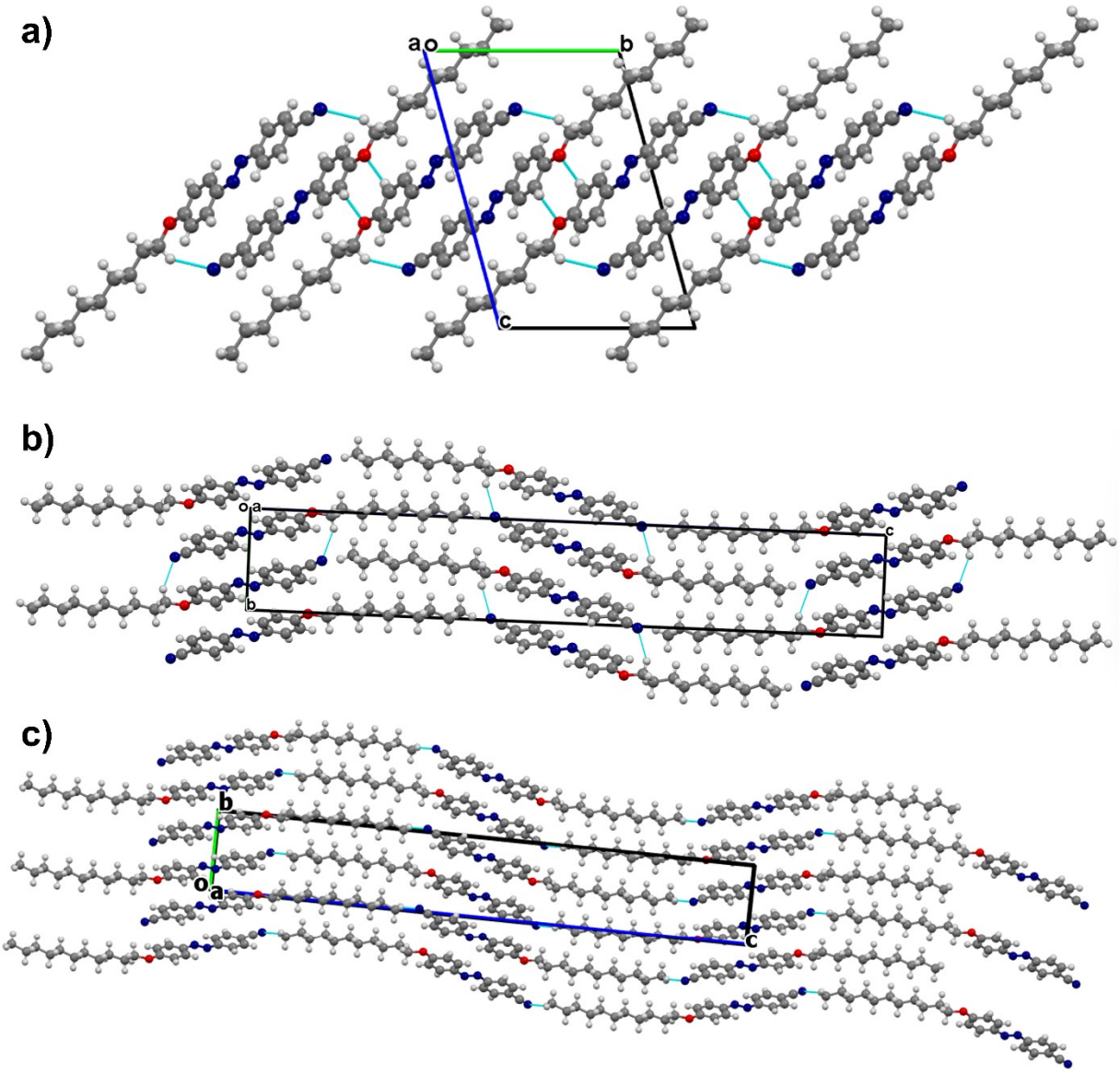

Fig. S9. Propagation of molecules in the crystal packing for a) **AZN-9**, b) **AZN-10** and c) **AZN-11** through the weak interactions such as C-H···N/O and π···π interactions, when viewed along a axis.

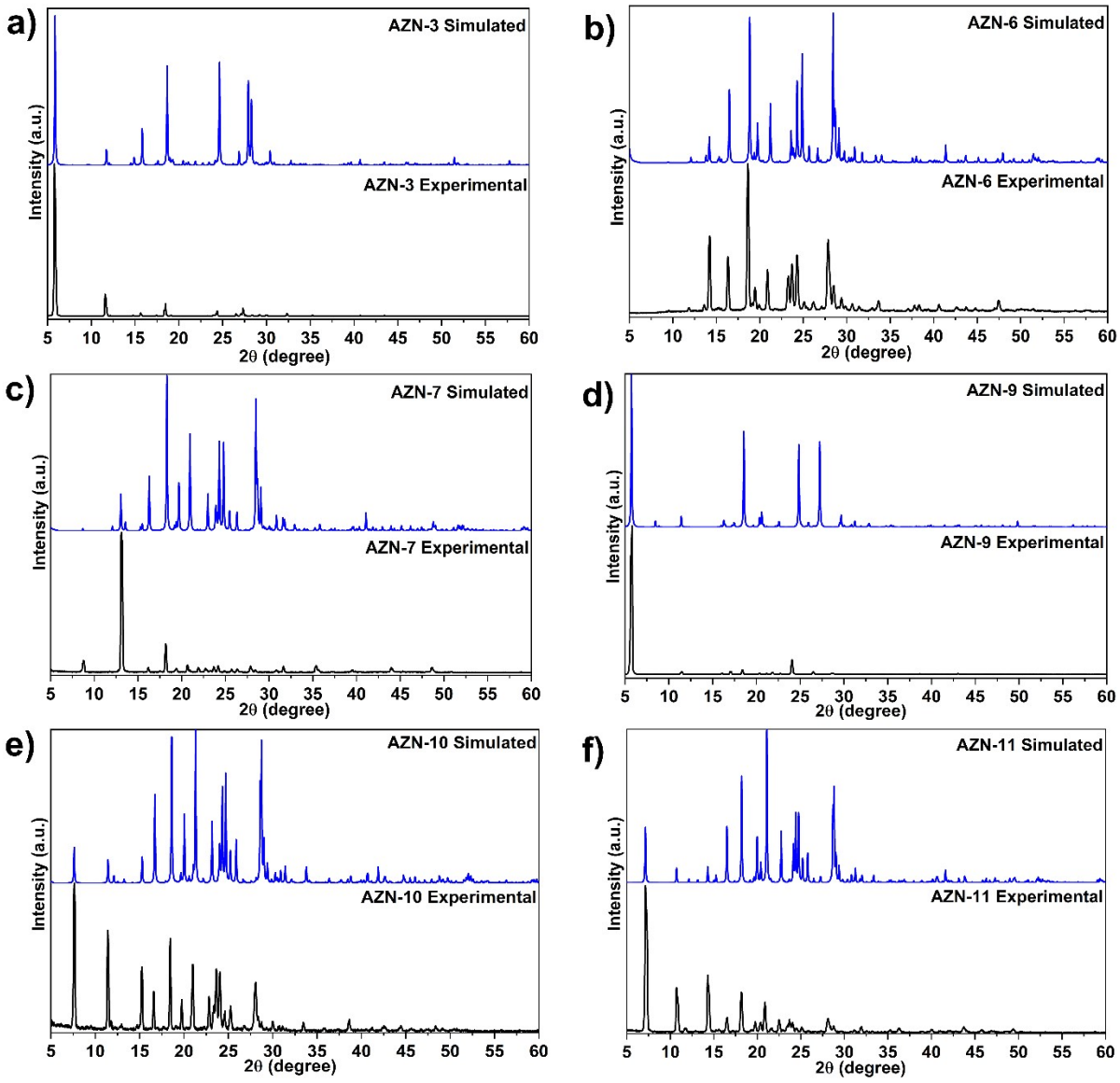

Fig. S10. Comparison between experimental and simulated PXRD patterns for a-f) **AZN-n** (**n= 3, 6, 7, 9, 10 and 11**).

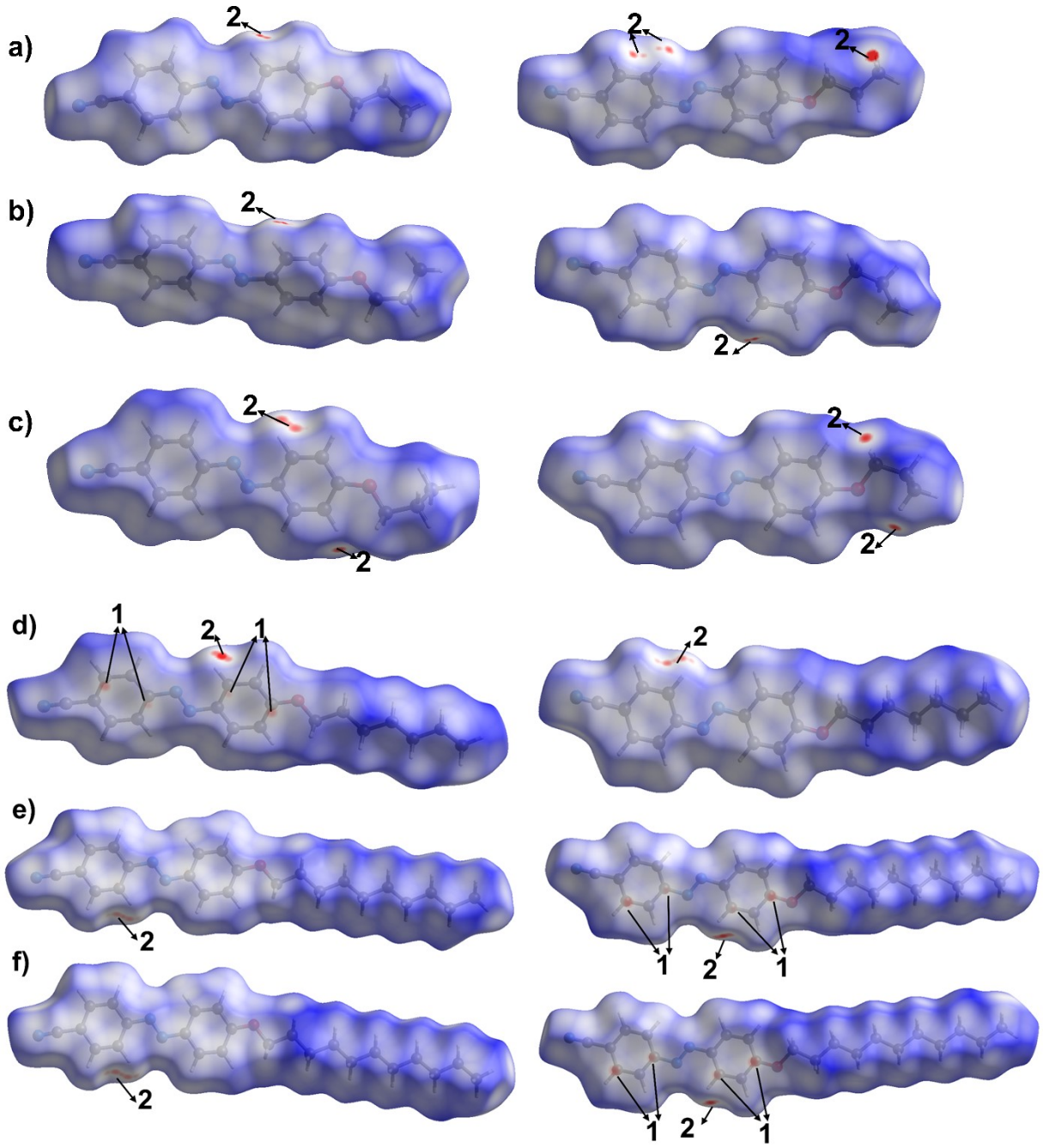

Fig. S11. d_{norm} mapped on HS surface; front view (left) and back view (right) for a-c) **AZN-3 (unit: A, B and C)**, d) **AZN-7**, e) **AZN-10** and f) **AZN-11**.

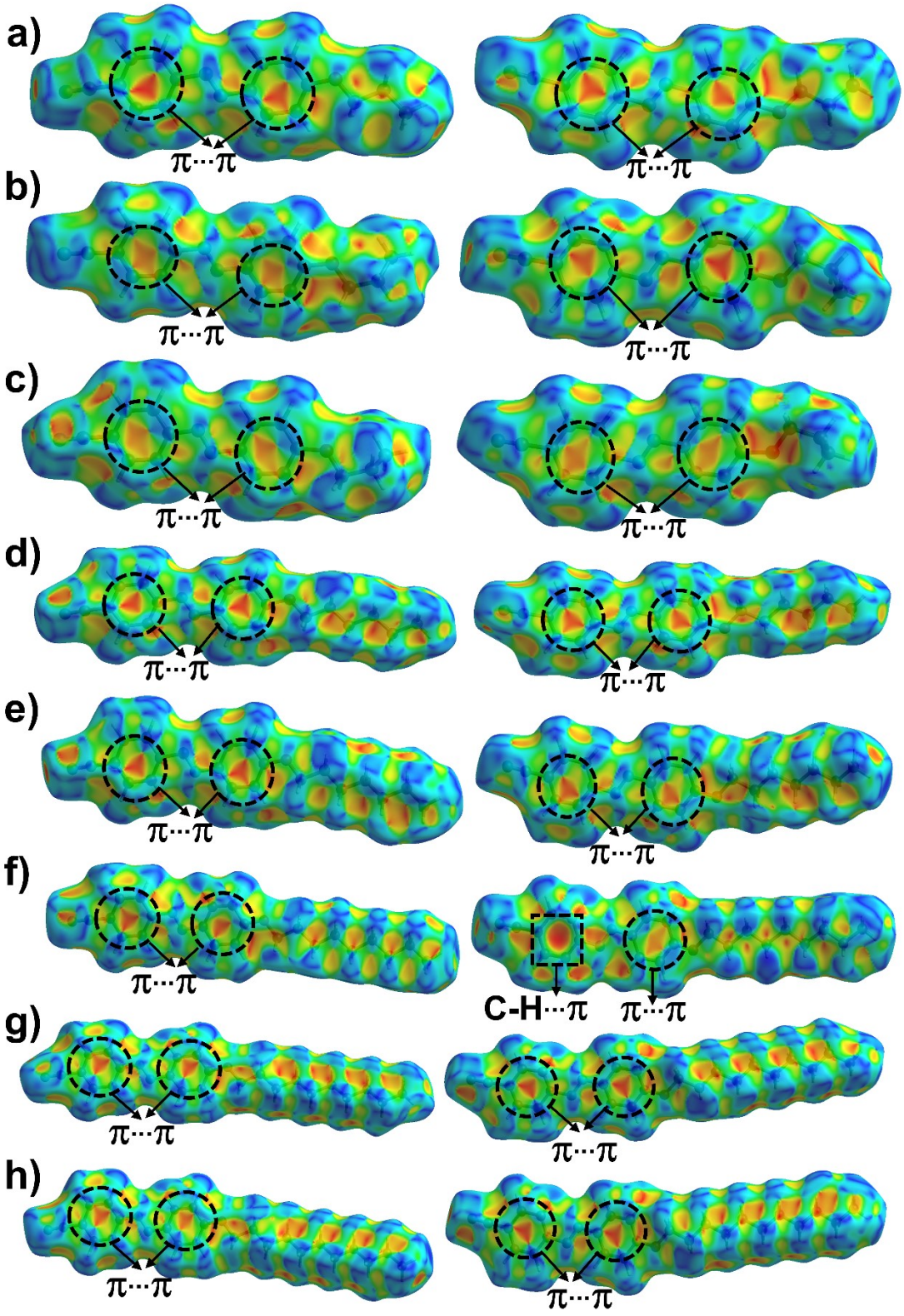

Fig. S12. Shape index mapped on HS surface; front view (left) and back view (right) for a-c) **AZN-3 (unit: A, B and C)**, d) **AZN-6**, e) **AZN-7**, f) **AZN-9**, g) **AZN-10** and h) **AZN-11**.

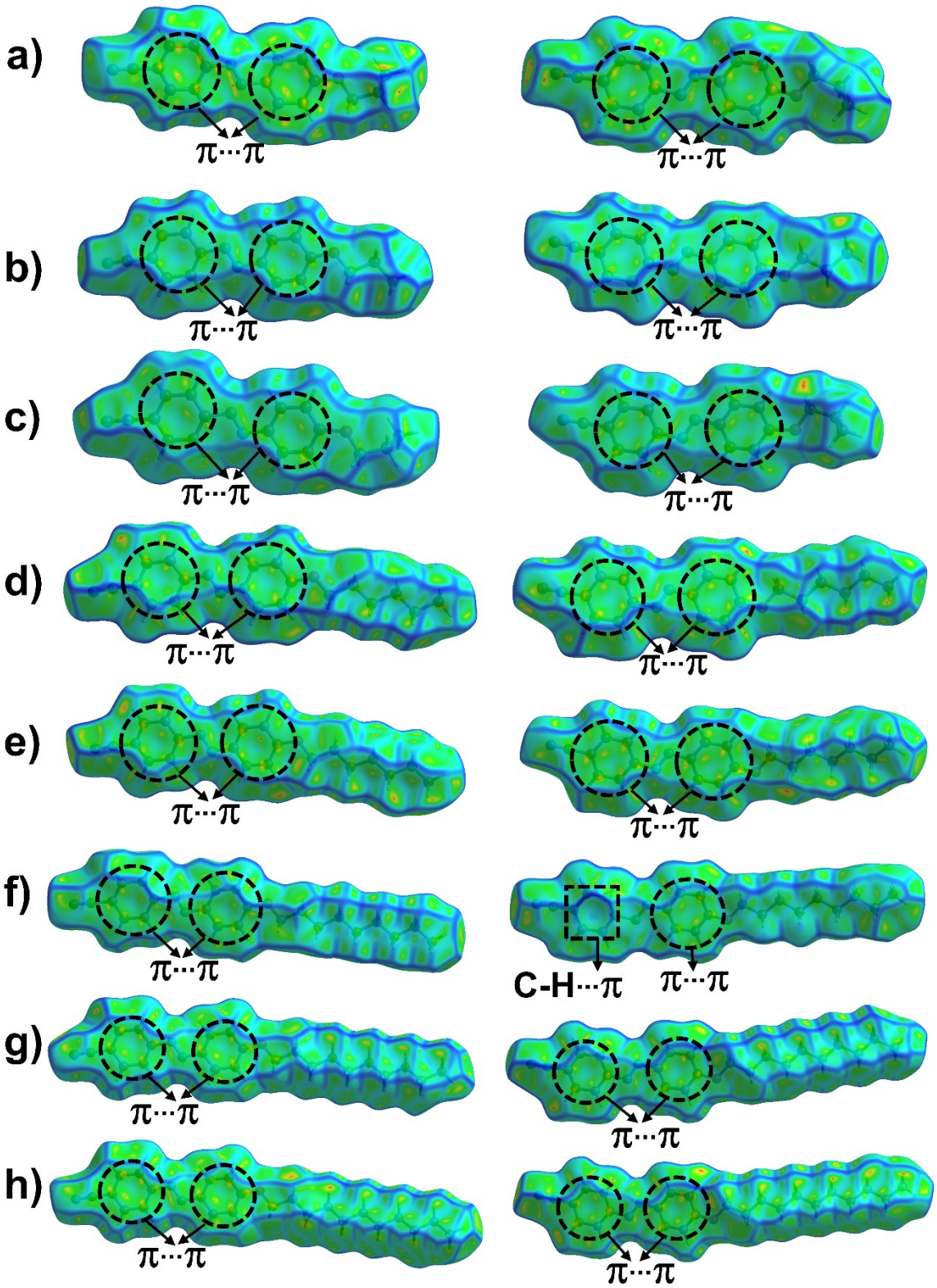

Fig. S13. Curvedness surface mapped on HS surface; front view (left) and back view (right) for a-c) **AZN-3 (unit: A, B and C)**, d) **AZN-6**, e) **AZN-7**, f) **AZN-9**, g) **AZN-10** and h) **AZN-11**.

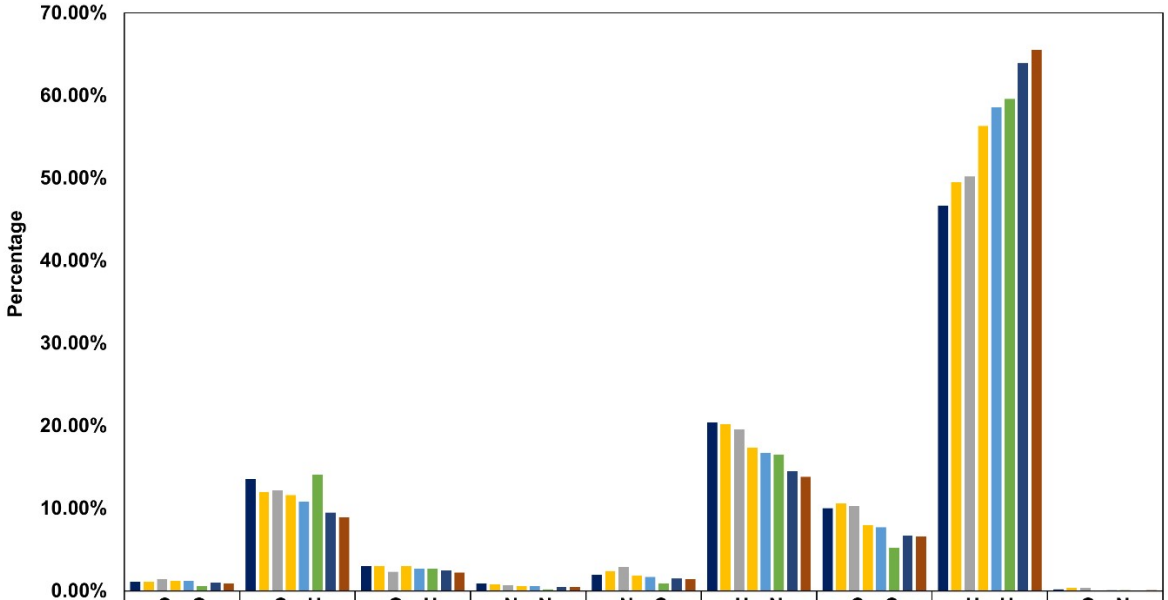

	C…O	C…H	O…H	N…N	N…C	H…N	C…C	H…H	O…N
AZN-3 A	1.10%	13.60%	3.00%	0.90%	2.00%	20.40%	10.00%	46.70%	0.20%
AZN-3 B	1.10%	12.00%	3.00%	0.80%	2.40%	20.20%	10.60%	49.50%	0.40%
AZN-3 C	1.40%	12.20%	2.30%	0.70%	2.90%	19.60%	10.30%	50.20%	0.40%
AZN-6	1.20%	11.60%	3.00%	0.60%	1.90%	17.40%	8.00%	56.30%	0.00%
AZN-7	1.20%	10.80%	2.70%	0.60%	1.70%	16.70%	7.70%	58.60%	0.10%
AZN-9	0.60%	14.10%	2.70%	0.20%	0.90%	16.50%	5.20%	59.60%	0.10%
AZN-10	1.00%	9.50%	2.50%	0.50%	1.50%	14.50%	6.70%	63.90%	0.00%
AZN-11	0.90%	8.90%	2.20%	0.50%	1.40%	13.80%	6.60%	65.50%	0.10%

Fig. S14. Bar diagram for percentage contribution in HS 2D finger print plot.

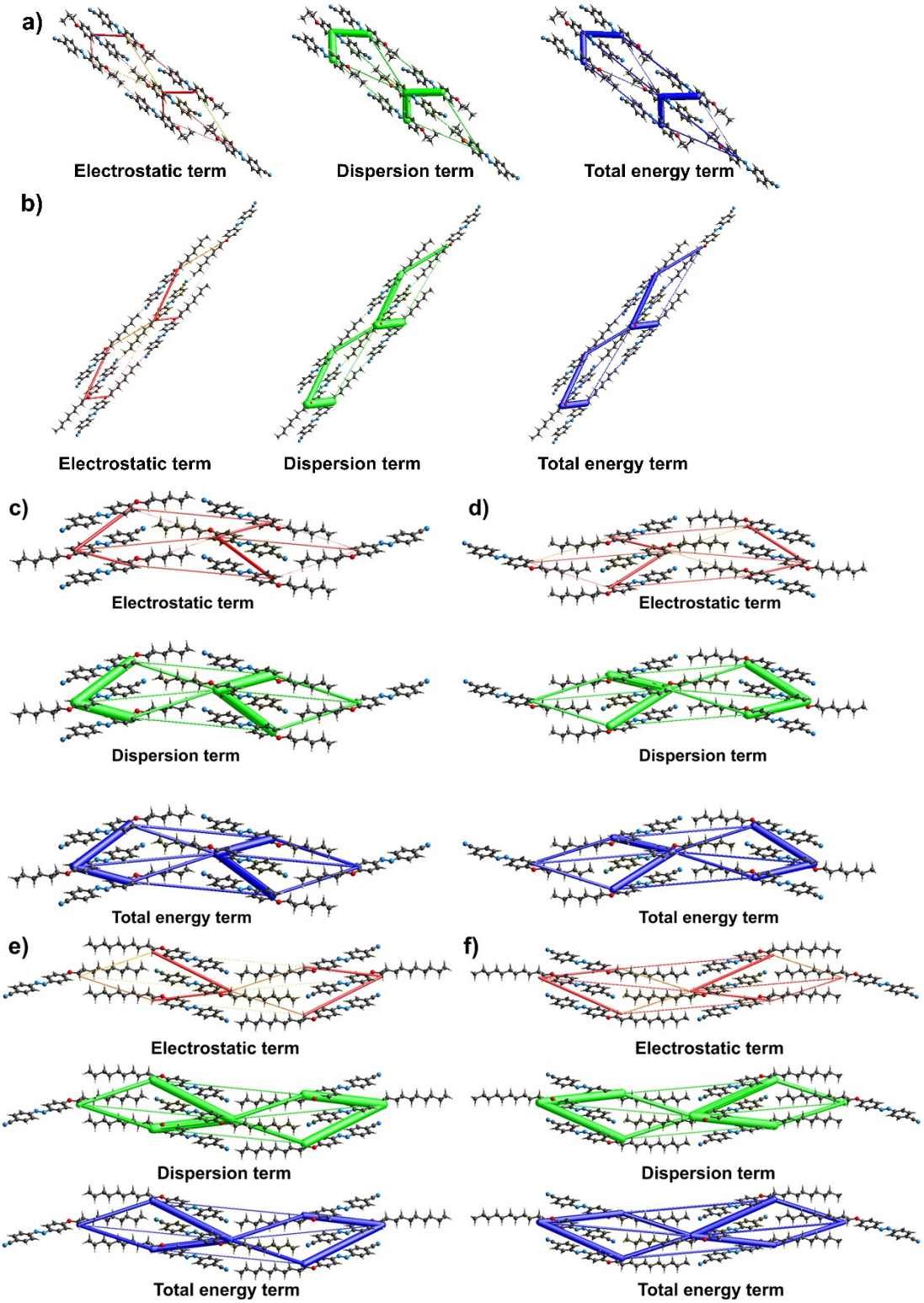

Fig. S15. Energy framework of different energy components for a) **AZN-3**, b) **AZN-9**, c) **AZN-6**, d) **AZN-7**, e) **AZN-10** and f) **AZN-11**, when observed along a axis.

Table S5. The pairwise intermolecular interaction energies for **AZN-n (n= 3, 6, 7, 9, 10 and 11)**

Interaction Energies is in kJ/mol.
R is the distance between molecular centroids (mean atomic position) in Å.
Total energies, only reported for the benchmarked energy models, are the sum of the four energy components, scaled appropriately (see the scale factor table below)
Scale factors for benchmarked energy model:

Energy Model	k_ele	k_pol	k_disp	k_rep
CE-B3LYP ... B3LYP/6-31G(d,p) electron densities	1.057	0.740	0.871	0.618

AZN-3 (A)

	N	Symop	R	Electron Density	E_ele	E_pol	E_dis	E_rep	E_tot
	0	-x, -y, -z	13.43	B3LYP/6-31G(d,p)	6.9	-1.4	-17.3	0.0	-8.8
	0	-	8.31	B3LYP/6-31G(d,p)	-15.5	-3.0	-27.9	21.7	-29.5
	0	-	4.76	B3LYP/6-31G(d,p)	-12.5	-4.1	-74.9	46.9	-52.5
	0	x, y, z	5.95	B3LYP/6-31G(d,p)	-6.2	-2.1	-42.5	26.3	-28.9
	1	-	3.87	B3LYP/6-31G(d,p)	-10.4	-2.9	-80.0	50.7	-51.5
	0	-	15.73	B3LYP/6-31G(d,p)	1.5	-0.3	-6.1	0.0	-4.0
	0	-	16.08	B3LYP/6-31G(d,p)	-6.5	-2.1	-11.3	0.0	-18.3
	1	-	6.10	B3LYP/6-31G(d,p)	-11.4	-1.5	-35.3	27.7	-26.7
	1	-	16.96	B3LYP/6-31G(d,p)	-2.8	-1.1	-7.3	0.0	-10.1
	0	-x, -y, -z	16.37	B3LYP/6-31G(d,p)	0.8	-0.2	-4.3	0.0	-3.0
	0	-	18.28	B3LYP/6-31G(d,p)	-2.7	-0.1	-6.8	0.0	-8.8
	0	-	18.89	B3LYP/6-31G(d,p)	-6.6	-1.8	-3.8	0.0	-11.6
	1	-	19.66	B3LYP/6-31G(d,p)	-2.1	-1.5	-2.8	0.0	-5.7

	2	x, y, z	5.95	B3LYP/6-31G(d,p)	-5.1	-1.9	-41.2	26.5	-26.3
	1	-x, -y, -z	4.67	B3LYP/6-31G(d,p)	-18.9	-4.9	-75.8	51.4	-57.9
	1	-x, -y, -z	16.04	B3LYP/6-31G(d,p)	2.3	-0.5	-6.8	0.0	-3.9
	1	-x, -y, -z	18.53	B3LYP/6-31G(d,p)	2.6	-0.3	-8.6	0.0	-4.9
	1	-	14.30	B3LYP/6-31G(d,p)	6.2	-0.9	-11.9	0.0	-4.5
	1	-	17.11	B3LYP/6-31G(d,p)	1.8	-0.1	-5.5	0.0	-3.0
	1	-	16.61	B3LYP/6-31G(d,p)	-5.4	-1.4	-7.6	0.0	-13.3
	1	-x, -y, -z	8.29	B3LYP/6-31G(d,p)	-19.0	-3.5	-30.6	28.0	-32.0
	1	-	19.38	B3LYP/6-31G(d,p)	-1.2	-1.8	-3.1	0.0	-5.3
	0	x, y, z	5.95	B3LYP/6-31G(d,p)	-8.0	-1.9	-40.4	28.5	-27.5
	0	-x, -y, -z	6.18	B3LYP/6-31G(d,p)	-11.4	-1.4	-31.0	24.7	-24.8
	0	-x, -y, -z	3.80	B3LYP/6-31G(d,p)	-9.2	-2.2	-78.6	48.7	-49.7

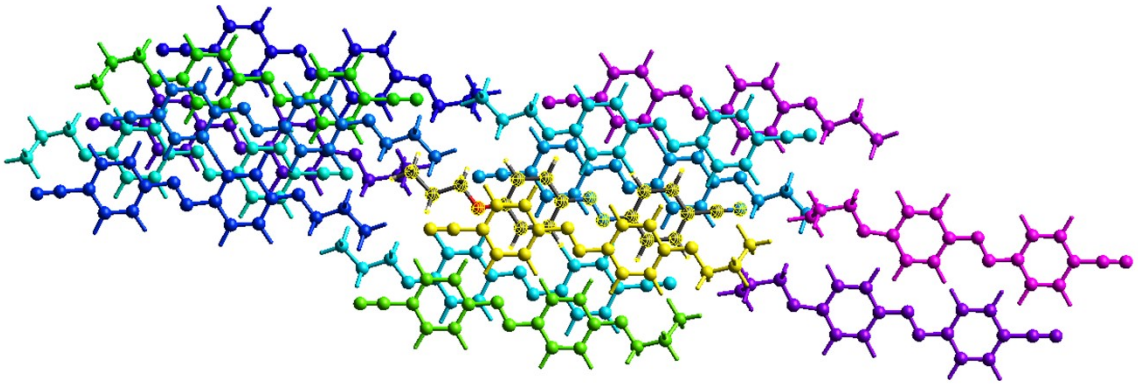

AZN-3 (B)

	N	Symop	R	Electron Density	E_ele	E_pol	E_dis	E_rep	E_tot
	1	-x, -y, -z	13.43	B3LYP/6-31G(d,p)	6.9	-1.4	-17.3	0.0	-8.8
	1	-	8.31	B3LYP/6-31G(d,p)	-15.5	-3.0	-27.9	21.7	-29.5
	1	-	4.76	B3LYP/6-31G(d,p)	-12.5	-4.1	-74.9	46.9	-52.5
	2	x, y, z	5.95	B3LYP/6-31G(d,p)	-6.2	-2.1	-42.5	26.3	-28.9
	1	-	3.87	B3LYP/6-31G(d,p)	-10.4	-2.9	-80.0	50.7	-51.5
	1	-	15.73	B3LYP/6-31G(d,p)	1.5	-0.3	-6.1	0.0	-4.0
	1	-	16.08	B3LYP/6-31G(d,p)	-6.5	-2.1	-11.3	0.0	-18.3
	1	-	6.10	B3LYP/6-31G(d,p)	-11.4	-1.5	-35.3	27.7	-26.7
	1	-	16.96	B3LYP/6-31G(d,p)	-2.8	-1.1	-7.3	0.0	-10.1
	1	-x, -y, -z	16.37	B3LYP/6-31G(d,p)	0.8	-0.2	-4.3	0.0	-3.0
	1	-	18.28	B3LYP/6-31G(d,p)	-2.7	-0.1	-6.8	0.0	-8.8
	1	-	18.89	B3LYP/6-31G(d,p)	-6.6	-1.8	-3.8	0.0	-11.6
	1	-	19.66	B3LYP/6-31G(d,p)	-2.1	-1.5	-2.8	0.0	-5.7
	0	x, y, z	5.95	B3LYP/6-31G(d,p)	-5.1	-1.9	-41.2	26.5	-26.3
	0	-x, -y, -z	4.67	B3LYP/6-31G(d,p)	-18.9	-4.9	-75.8	51.4	-57.9
	0	-x, -y, -z	16.04	B3LYP/6-31G(d,p)	2.3	-0.5	-6.8	0.0	-3.9
	0	-x, -y, -z	18.53	B3LYP/6-31G(d,p)	2.6	-0.3	-8.6	0.0	-4.9
	0	-	14.30	B3LYP/6-31G(d,p)	6.2	-0.9	-11.9	0.0	-4.5
	0	-	17.11	B3LYP/6-31G(d,p)	1.8	-0.1	-5.5	0.0	-3.0
	0	-	16.61	B3LYP/6-31G(d,p)	-5.4	-1.4	-7.6	0.0	-13.3

	0	-x, -y, -z	8.29	B3LYP/6-31G(d,p)	-19.0	-3.5	-30.6	28.0	-32.0
	0	-	19.38	B3LYP/6-31G(d,p)	-1.2	-1.8	-3.1	0.0	-5.3
	0	x, y, z	5.95	B3LYP/6-31G(d,p)	-8.0	-1.9	-40.4	28.5	-27.5
	0	-x, -y, -z	6.18	B3LYP/6-31G(d,p)	-11.4	-1.4	-31.0	24.7	-24.8
	0	-x, -y, -z	3.80	B3LYP/6-31G(d,p)	-9.2	-2.2	-78.6	48.7	-49.7

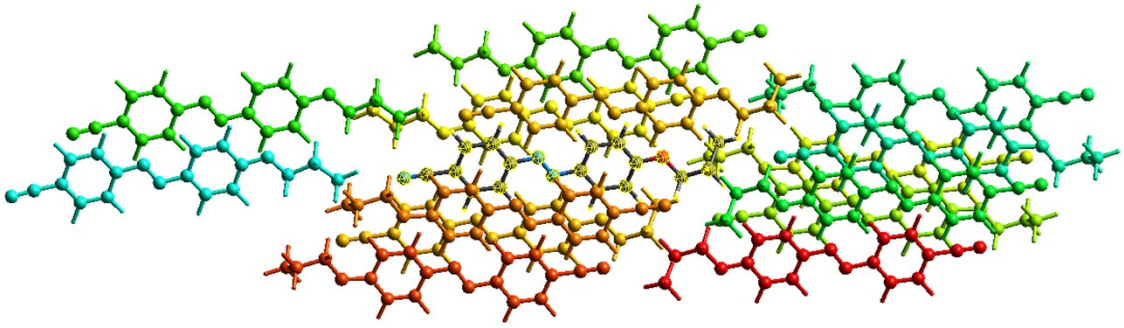

AZN-3 (C)

	N	Symop	R	Electron Density	E_ele	E_pol	E_dis	E_rep	E_tot
	0	-x, -y, -z	13.43	B3LYP/6-31G(d,p)	6.9	-1.4	-17.3	0.0	-8.8
	1	-	8.31	B3LYP/6-31G(d,p)	-15.5	-3.0	-27.9	21.7	-29.5
	1	-	4.76	B3LYP/6-31G(d,p)	-12.5	-4.1	-74.9	46.9	-52.5
	0	x, y, z	5.95	B3LYP/6-31G(d,p)	-6.2	-2.1	-42.5	26.3	-28.9
	0	-	3.87	B3LYP/6-31G(d,p)	-10.4	-2.9	-80.0	50.7	-51.5
	1	-	15.73	B3LYP/6-31G(d,p)	1.5	-0.3	-6.1	0.0	-4.0
	1	-	16.08	B3LYP/6-31G(d,p)	-6.5	-2.1	-11.3	0.0	-18.3
	0	-	6.10	B3LYP/6-31G(d,p)	-11.4	-1.5	-35.3	27.7	-26.7
	0	-	16.96	B3LYP/6-31G(d,p)	-2.8	-1.1	-7.3	0.0	-10.1

	0	-x, -y, -z	16.37	B3LYP/6-31G(d,p)	0.8	-0.2	-4.3	0.0	-3.0
	1	-	18.28	B3LYP/6-31G(d,p)	-2.7	-0.1	-6.8	0.0	-8.8
	1	-	18.89	B3LYP/6-31G(d,p)	-6.6	-1.8	-3.8	0.0	-11.6
	0	-	19.66	B3LYP/6-31G(d,p)	-2.1	-1.5	-2.8	0.0	-5.7
	0	x, y, z	5.95	B3LYP/6-31G(d,p)	-5.1	-1.9	-41.2	26.5	-26.3
	0	-x, -y, -z	4.67	B3LYP/6-31G(d,p)	-18.9	-4.9	-75.8	51.4	-57.9
	0	-x, -y, -z	16.04	B3LYP/6-31G(d,p)	2.3	-0.5	-6.8	0.0	-3.9
	0	-x, -y, -z	18.53	B3LYP/6-31G(d,p)	2.6	-0.3	-8.6	0.0	-4.9
	1	-	14.30	B3LYP/6-31G(d,p)	6.2	-0.9	-11.9	0.0	-4.5
	1	-	17.11	B3LYP/6-31G(d,p)	1.8	-0.1	-5.5	0.0	-3.0
	1	-	16.61	B3LYP/6-31G(d,p)	-5.4	-1.4	-7.6	0.0	-13.3
	0	-x, -y, -z	8.29	B3LYP/6-31G(d,p)	-19.0	-3.5	-30.6	28.0	-32.0
	1	-	19.38	B3LYP/6-31G(d,p)	-1.2	-1.8	-3.1	0.0	-5.3
	2	x, y, z	5.95	B3LYP/6-31G(d,p)	-8.0	-1.9	-40.4	28.5	-27.5
	1	-x, -y, -z	6.18	B3LYP/6-31G(d,p)	-11.4	-1.4	-31.0	24.7	-24.8
	1	-x, -y, -z	3.80	B3LYP/6-31G(d,p)	-9.2	-2.2	-78.6	48.7	-49.7

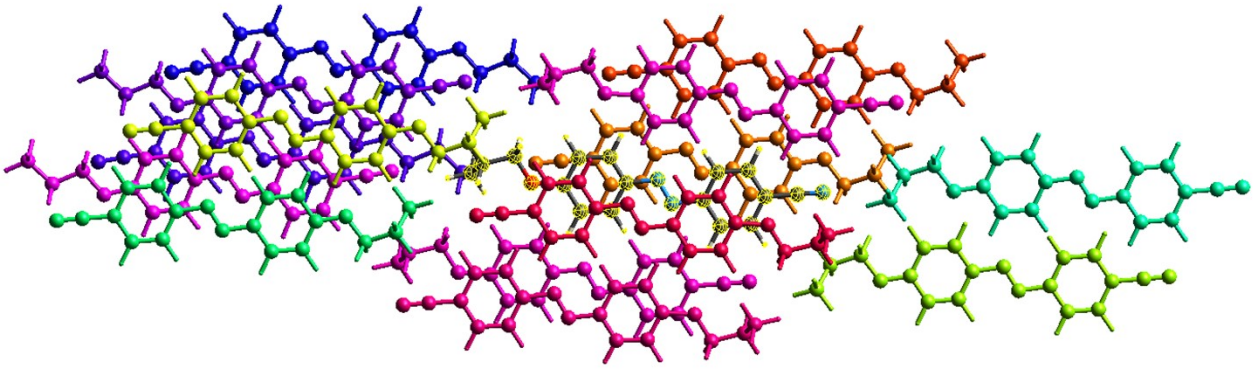

AZN-6:

	N	Symop	R	Electron Density	E_ele	E_pol	E_dis	E_rep	E_tot
	1	-x, -y, -z	6.99	B3LYP/6-31G(d,p)	-20.4	-4.6	-77.3	56.7	-57.2
	1	-x, -y, -z	10.58	B3LYP/6-31G(d,p)	-18.0	-3.4	-30.1	27.0	-31.0
	2	x+1/2, -y+1/2, z+1/2	20.27	B3LYP/6-31G(d,p)	-6.6	-1.6	-9.4	0.0	-16.4
	2	x, y, z	5.81	B3LYP/6-31G(d,p)	-6.1	-2.3	-50.8	32.8	-32.1
	1	-x, -y, -z	5.74	B3LYP/6-31G(d,p)	-13.4	-3.1	-83.9	58.2	-53.6
	2	-x+1/2, y+1/2, -z+1/2	15.66	B3LYP/6-31G(d,p)	-1.5	-0.7	-21.5	0.0	-20.8
	1	-x, -y, -z	6.11	B3LYP/6-31G(d,p)	-14.1	-1.6	-35.5	29.7	-28.8
	2	x+1/2, -y+1/2, z+1/2	23.12	B3LYP/6-31G(d,p)	-0.1	-1.5	-2.6	0.0	-3.4
	2	-x+1/2, y+1/2, -z+1/2	18.43	B3LYP/6-31G(d,p)	-0.6	-0.2	-15.7	0.0	-14.4

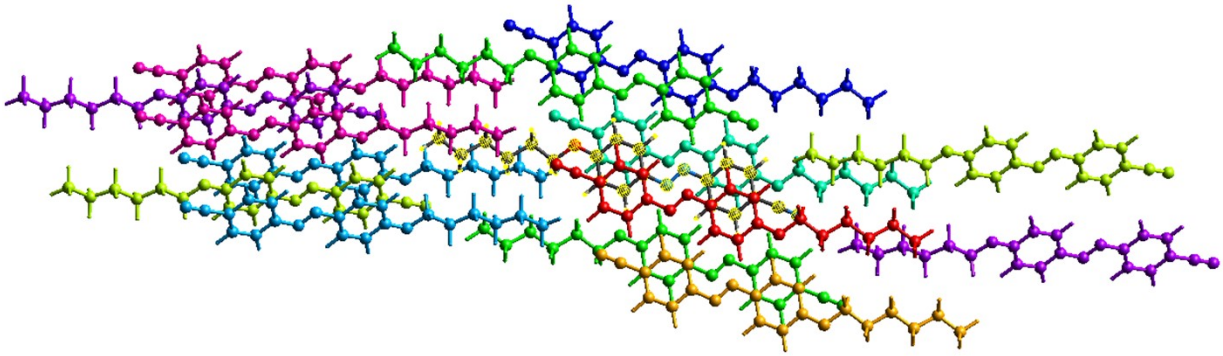

AZN-7

	N	Symop	R	Electron Density	E_ele	E_pol	E_dis	E_rep	E_tot
	2	-x+1/2, y+1/2, -z+1/2	18.78	B3LYP/6-31G(d,p)	1.8	-0.2	-18.3	0.0	-14.1
	2	x, y, z	5.82	B3LYP/6-31G(d,p)	-6.6	-2.3	-50.6	31.8	-33.1
	1	-x, -y, -z	7.75	B3LYP/6-31G(d,p)	-18.4	-4.4	-78.0	55.2	-56.5
	2	-x+1/2, y+1/2, -z+1/2	16.16	B3LYP/6-31G(d,p)	-2.4	-0.6	-20.7	0.0	-21.0
	1	-x, -y, -z	6.75	B3LYP/6-31G(d,p)	-11.3	-1.3	-30.6	23.2	-25.2
	2	x+1/2, -y+1/2, z+1/2	21.80	B3LYP/6-31G(d,p)	-4.3	-1.3	-8.9	0.0	-13.3
	1	-x, -y, -z	6.64	B3LYP/6-31G(d,p)	-12.5	-2.7	-83.1	57.9	-51.9
	1	-x, -y, -z	11.25	B3LYP/6-31G(d,p)	-18.8	-3.7	-32.1	29.6	-32.3
	2	x+1/2, -y+1/2, z+1/2	24.47	B3LYP/6-31G(d,p)	-4.9	-1.5	-2.6	0.0	-8.6

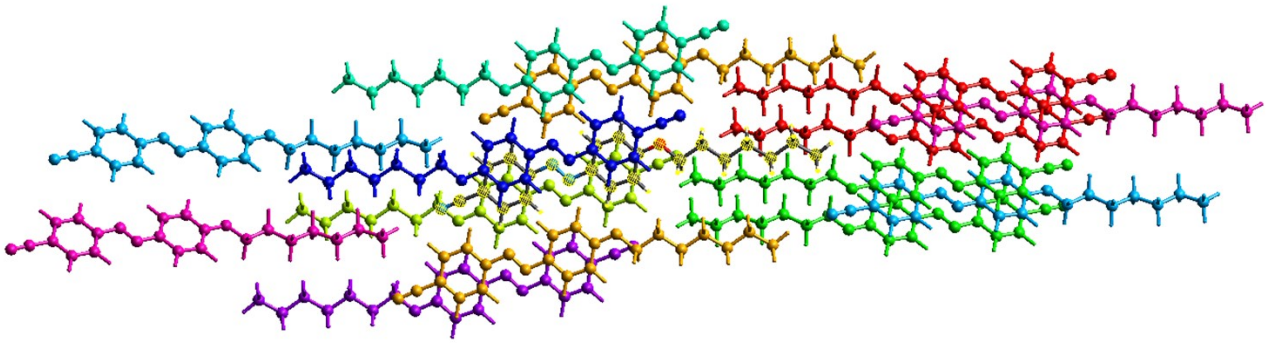

AZN-9

	N	Symop	R	Electron Density	E_ele	E_pol	E_dis	E_rep	E_tot
	2	x, y, z	5.82	B3LYP/6-31G(d,p)	-5.7	-2.2	-54.6	30.9	-36.1
	1	-x, -y, -z	13.47	B3LYP/6-31G(d,p)	-21.9	-3.3	-30.0	0.0	-51.7
	1	-x, -y, -z	10.00	B3LYP/6-31G(d,p)	-20.8	-4.9	-75.1	55.4	-56.8
	1	-x, -y, -z	3.77	B3LYP/6-31G(d,p)	-17.0	-3.6	-114.0	71.6	-75.7
	1	-x, -y, -z	16.00	B3LYP/6-31G(d,p)	-4.1	-0.9	-31.5	0.0	-32.5
	1	-x, -y, -z	5.94	B3LYP/6-31G(d,p)	-14.7	-2.0	-50.8	39.2	-37.0
	1	-x, -y, -z	18.59	B3LYP/6-31G(d,p)	10.3	-0.4	-41.5	0.0	-25.5
	2	x, y, z	24.88	B3LYP/6-31G(d,p)	-3.6	-0.7	-4.7	0.0	-8.5
	1	-x, -y, -z	24.50	B3LYP/6-31G(d,p)	-0.7	-0.0	-2.7	0.0	-3.1
	2	x, y, z	27.50	B3LYP/6-31G(d,p)	0.4	-1.7	-2.9	0.0	-3.3
	1	-x, -y, -z	26.92	B3LYP/6-31G(d,p)	-1.4	-0.0	-7.2	0.0	-7.8

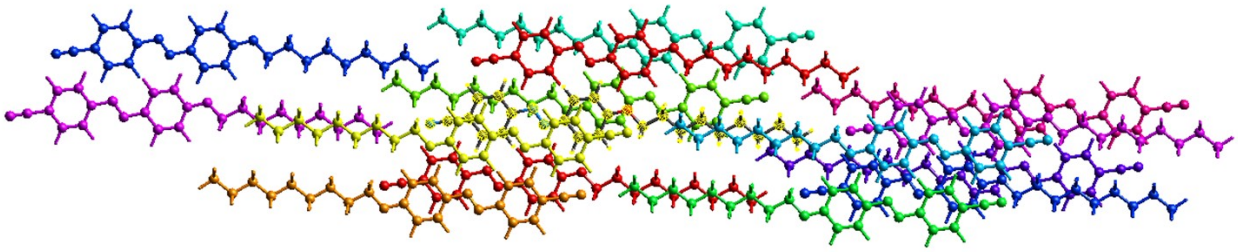

AZN-10

	N	Symop	R	Electron Density	E_ele	E_pol	E_dis	E_rep	E_tot
	2	-x, y+1/2, -z+1/2	19.31	B3LYP/6-31G(d,p)	-2.4	-0.2	-31.0	0.0	-29.7
	2	-x, y+1/2, -z+1/2	16.54	B3LYP/6-31G(d,p)	6.6	-0.7	-36.0	0.0	-24.9
	2	x, y, z	5.80	B3LYP/6-31G(d,p)	-7.9	-2.3	-61.0	39.1	-39.0
	2	x, -y+1/2, z+1/2	25.42	B3LYP/6-31G(d,p)	1.4	-1.6	-9.2	0.0	-7.6
	1	-x, -y, -z	8.47	B3LYP/6-31G(d,p)	-14.5	-1.7	-35.8	30.5	-28.9
	1	-x, -y, -z	9.58	B3LYP/6-31G(d,p)	-14.4	-3.1	-86.9	63.2	-54.2
	1	-x, -y, -z	10.70	B3LYP/6-31G(d,p)	-20.6	-4.6	-80.0	61.1	-57.1
	1	-x, -y, -z	14.20	B3LYP/6-31G(d,p)	-16.7	-3.4	-30.6	0.0	-46.8
	2	x, -y+1/2, z+1/2	28.27	B3LYP/6-31G(d,p)	0.6	-1.4	-2.6	0.0	-2.7

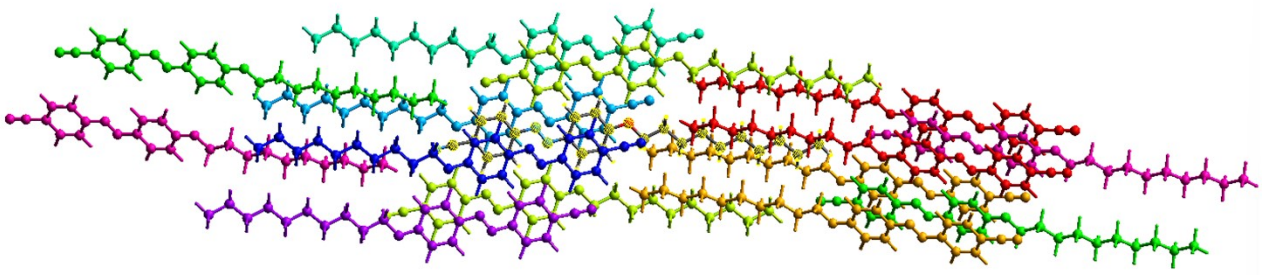

AZN-11

	N	Symop	R	Electron Density	E_ele	E_pol	E_dis	E_rep	E_tot
	2	x, y, z	5.81	B3LYP/6-31G(d,p)	-8.3	-2.4	-60.7	38.9	-39.3
	1	-x, -y, -z	10.66	B3LYP/6-31G(d,p)	-13.6	-2.9	-86.1	63.1	-52.5
	1	-x, -y, -z	15.04	B3LYP/6-31G(d,p)	-19.7	-3.9	-33.0	0.0	-52.4
	2	x, -y+1/2, z+1/2	26.83	B3LYP/6-31G(d,p)	-6.5	-1.4	-9.3	0.0	-16.1
	1	-x, -y, -z	11.66	B3LYP/6-31G(d,p)	-19.5	-4.6	-80.9	60.4	-57.2
	2	-x, y+1/2, -z+1/2	16.83	B3LYP/6-31G(d,p)	5.4	-0.7	-37.7	0.0	-27.5
	1	-x, -y, -z	9.53	B3LYP/6-31G(d,p)	-11.3	-1.3	-30.7	23.8	-25.0
	2	-x, y+1/2, -z+1/2	19.50	B3LYP/6-31G(d,p)	-7.8	-0.2	-33.6	0.0	-37.7
	2	x, -y+1/2, z+1/2	29.55	B3LYP/6-31G(d,p)	-1.9	-1.6	-2.8	0.0	-5.7

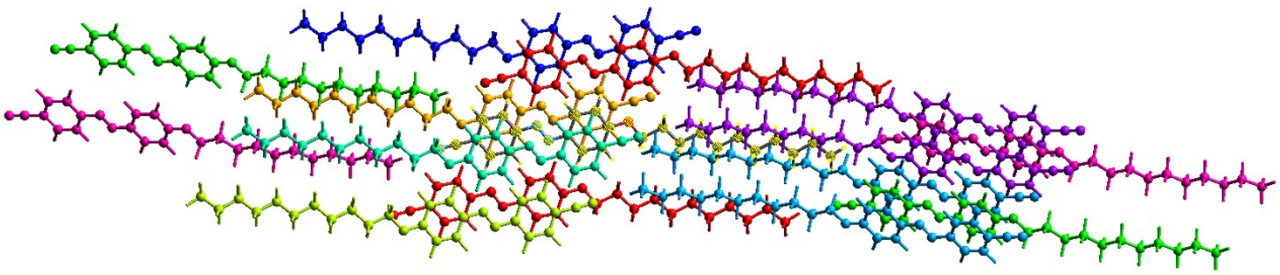

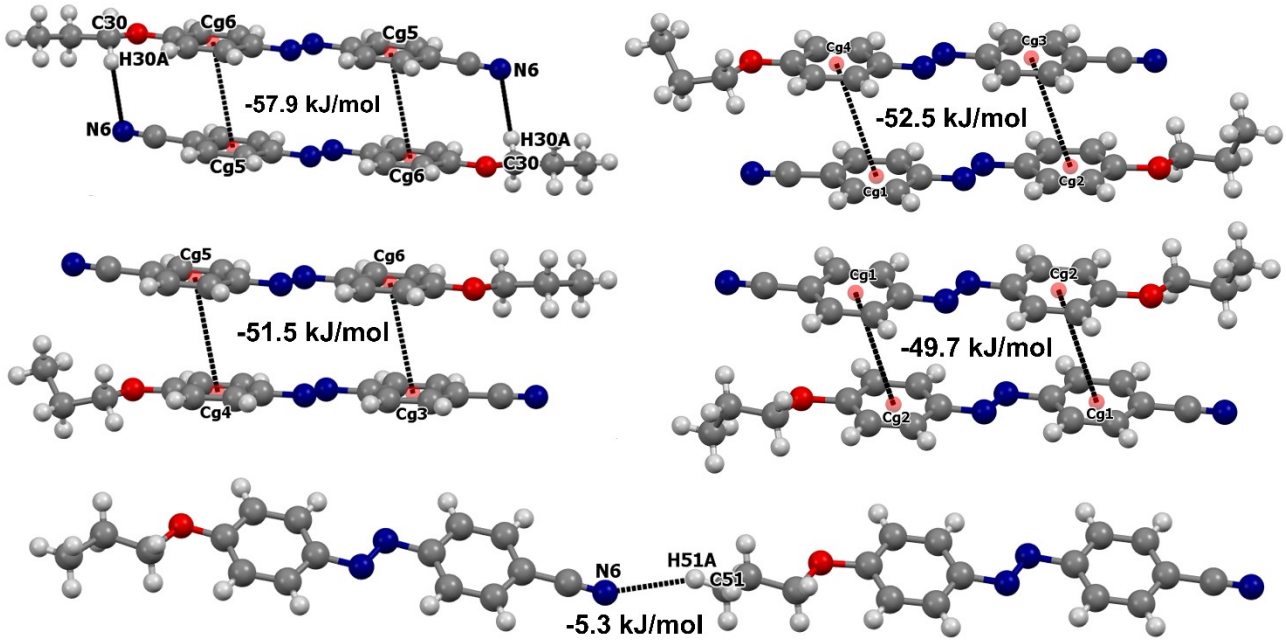

Fig. S16. Interaction energies for the molecular pairs in **AZN-3**.

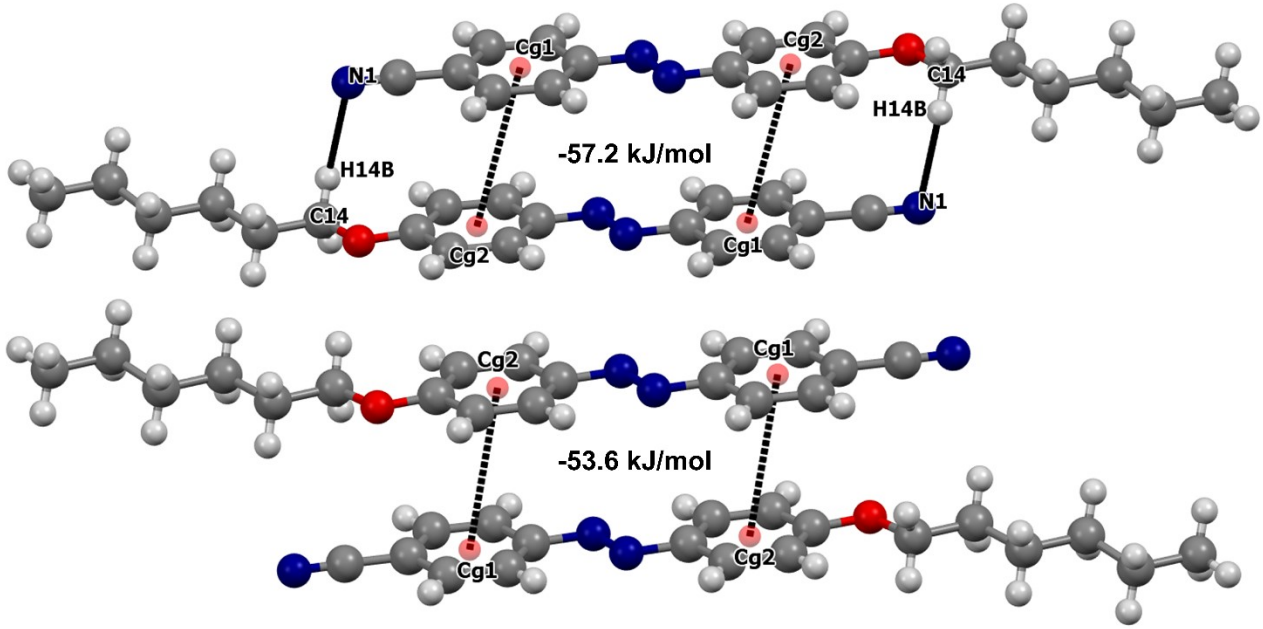

Fig. S17. Interaction energies for the molecular pairs in **AZN-6**.

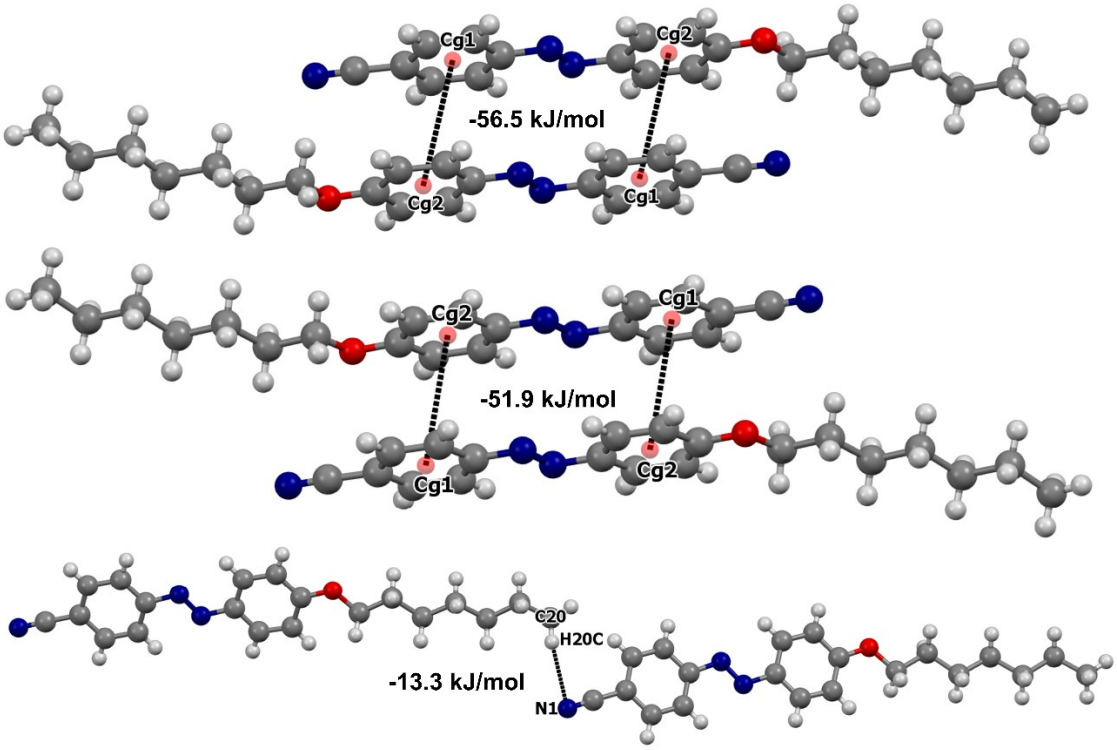

Fig. S18. Interaction energies for the molecular pairs in **AZN-7**.

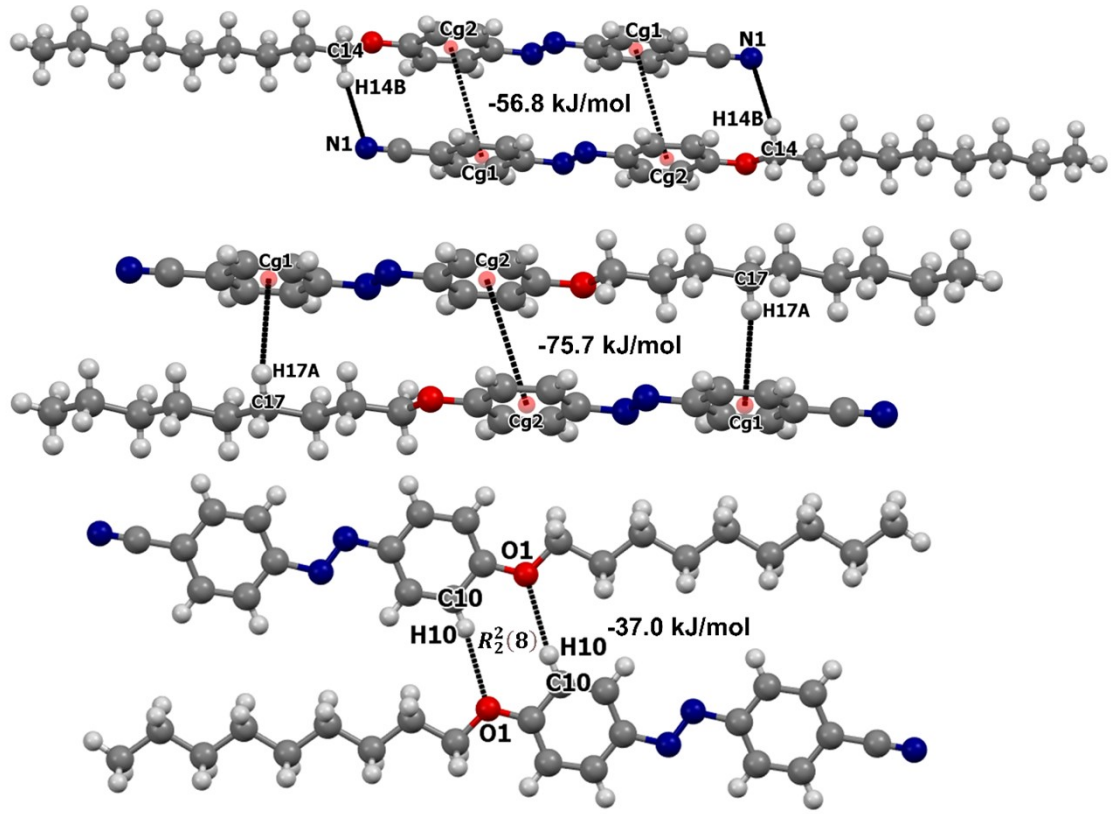

Fig. S19. Interaction energies for the molecular pairs in **AZN-9**.

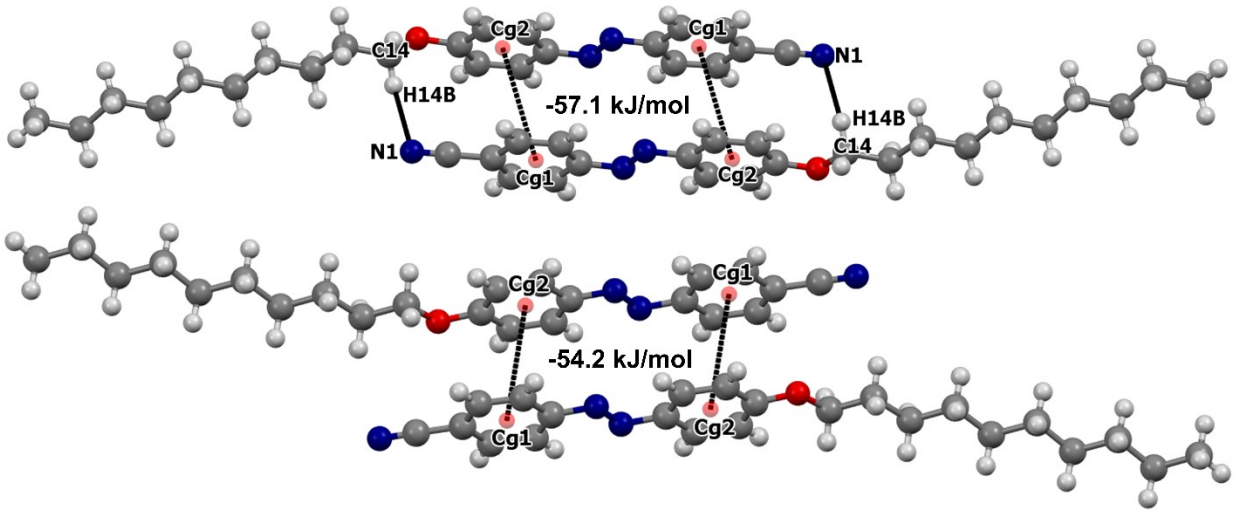

Fig. S20. Interaction energies for the molecular pairs in **AZN-10**.

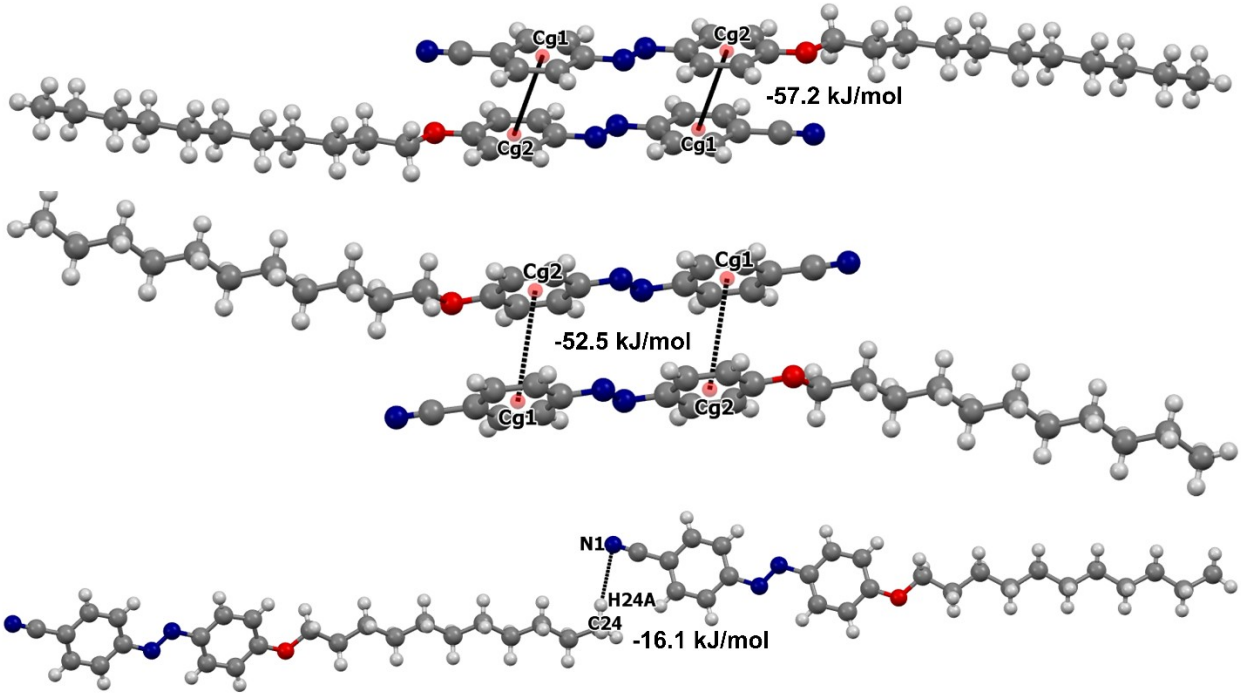

Fig. S21. Interaction energies for the molecular pairs in **AZN-11**.

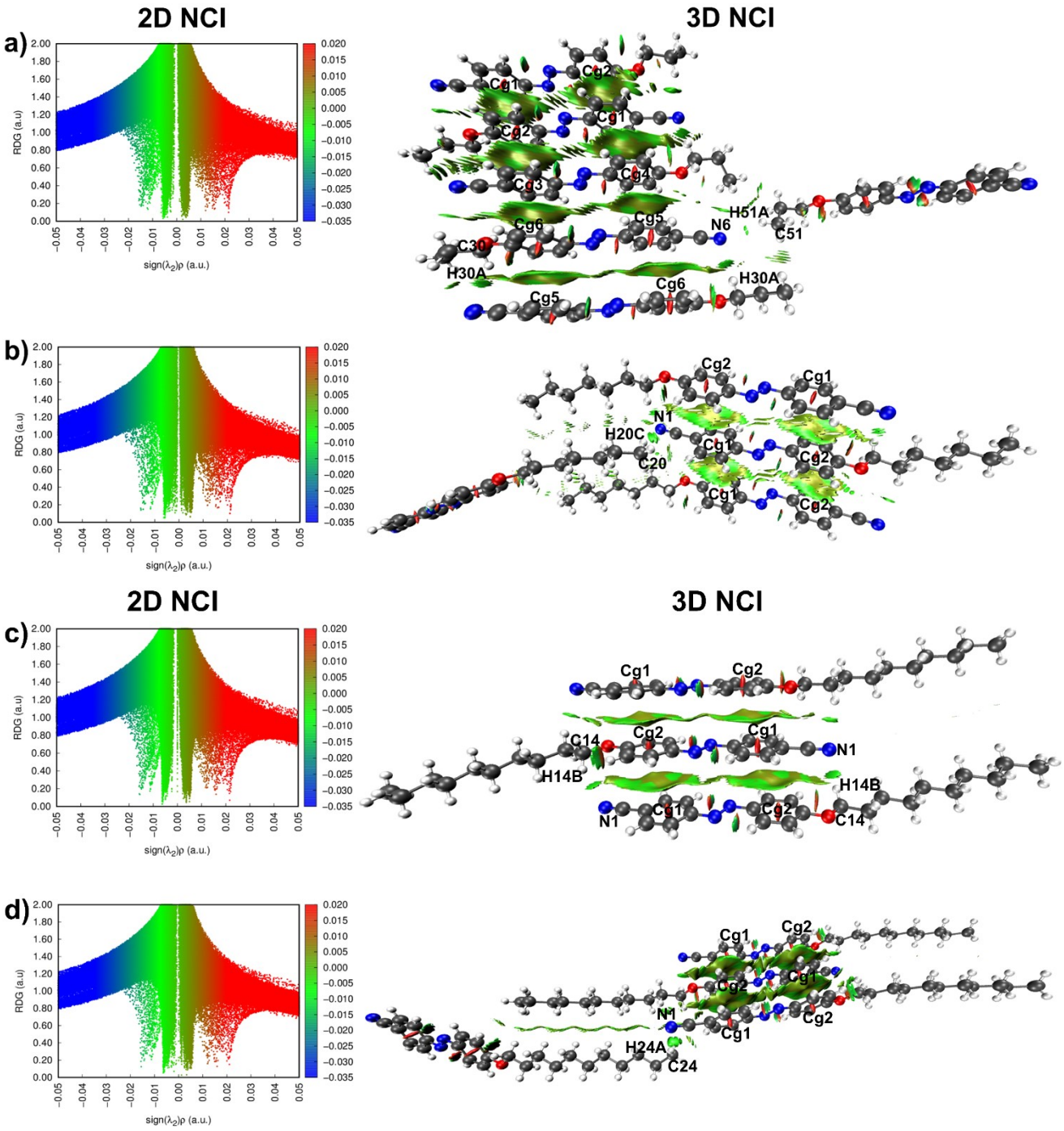

Fig. S22. 2D NCI scatterplot (left) and 3D gradient isosurface (right) for the crystal packing of the compounds, a) **AZN-3**, b) **AZN-7**, c) **AZN-10** and d) **AZN-11** showing C-H···N and Cg···Cg (π···π) weak contacts.

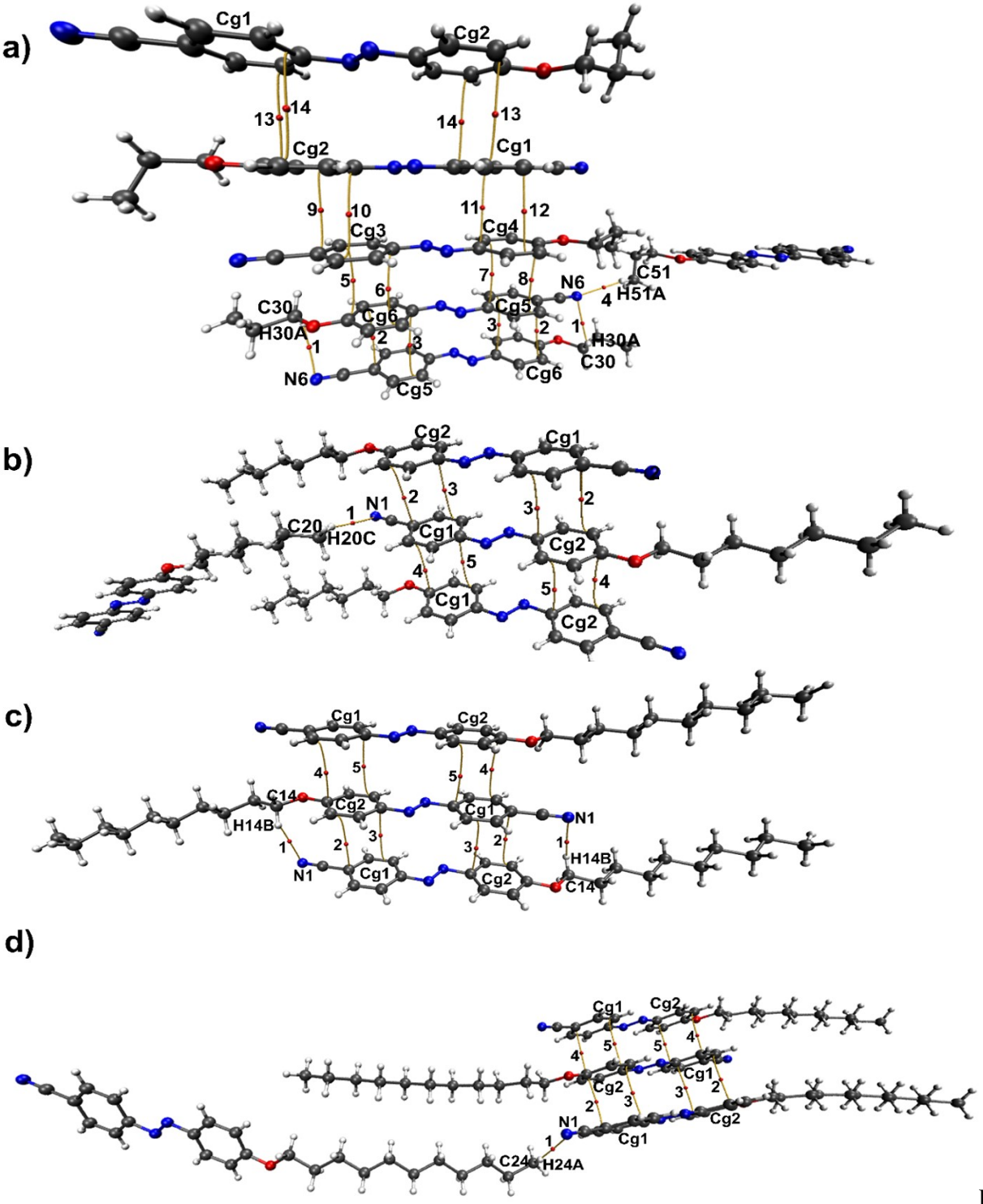

Fig. S23. BCPs (red dots) and BPs (orange line) showing the weak interactions such as C-H···N and Cg···Cg (π···π) interactions in **AZN-n** (**n=3, 7, 10 and 11**).

Table S6. Topological parameters for intermolecular interactions in **AZN-n** (**n = 3**, **6**, **7**, **9**, **10** and **11**) at their (3, −1) BCPs. ρ(r): electron density; $\nabla^2\rho(r)$: Laplacian of electron density; G(r): kinetic energy density; V(r): potential energy density; H(r): total electronic density; sign (λ_2) ρ (all units are a.u.); |V(r)|/G(r); distance (D) in Å.

Sample Code	Interaction	BCP no.	D	Sign(λ_2)ρ	ρ (r)	$\nabla^2\rho(r)$	G(r)	V(r)	H(r)	|V(r)|/G(r)
AZN-3	C30-H30A···N6	1	2.719	-0.0065	0.0065	0.0205	0.0043	-0.0034	0.0009	0.7970
	C51-H51A···N6	4	2.739	-0.0060	0.0060	0.0617	0.0140	-0.0131	0.0007	0.9357
	Cg1···Cg2	13	3.790	-0.0051	0.0051	0.0129	0.0027	-0.0021	0.0006	0.7778
		14		-0.0051	0.0051	0.0129	0.0027	-0.0021	0.0006	0.7778
	Cg2···Cg3	9	3.741	-0.0056	0.0056	0.0147	0.0030	-0.0024	0.0006	0.8000
		10		-0.0056	0.0056	0.0146	0.0030	-0.0024	0.0006/7	0.8000
	Cg1···Cg4	11	3.837	-0.0051	0.0051	0.0134	0.0028	-0.0022	0.0006	0.7857
		12		-0.0050	0.0050	0.0130	0.0027	-0.0022	0.0005	0.8148
	Cg3···Cg6	5	3.621	-0.0059	0.0059	0.0153	0.0031	-0.0024	0.0007	0.7742
		6		-0.0057	0.0057	0.0154	0.0032	-0.0025	0.0007	0.7813
	Cg4···Cg5	7	3.785	-0.0053	0.0053	0.0144	0.0030	-0.0023	0.0007	0.7667
		8		-0.0051	0.0051	0.0133	0.0027	-0.0021	0.0006	0.7778
	Cg5···Cg6	2	3.794	-0.0057	0.0057	0.0152	0.0032	-0.0025	0.0006	0.7813
		3		-0.0052	0.0052	0.0137	0.0028	-0.0022	0.0006	0.7857
AZN-6	C14-H14B···N1	1	2.718	-0.0063	0.0063	0.0187	0.0040	-0.0032	0.0007	0.8000
	Cg1···Cg2	2	3.801	-0.0059	0.0059	0.0156	0.0032	-0.0026	0.0007	0.8125
		3		-0.0060	0.0060	0.0161	0.0033	-0.0026	0.0007	0.7879
	Cg1···Cg2	4	3.672	-0.0061	0.0061	0.0172	0.0035	-0.0027	0.0008	0.7714
		5		-0.0059	0.0059	0.0161	0.0033	-0.0026	0.0007	0.7879
AZN-7	C20-H20C···N1	1	2.745	-0.0062	0.0062	0.0177	0.0037	-0.0030	0.0007	0.8108
	Cg1···Cg2	2	3.681	-0.0059	0.0059	0.0154	0.0032	-0.0026	0.0007	0.8125
		3		-0.0058	0.0058	0.0154	0.0032	-0.0026	0.0007	0.8125
	Cg1···Cg2	4	3.762	-0.0063	0.0063	0.0175	0.0035	-0.0027	0.0008	0.7714
		5		-0.0062	0.0062	0.0171	0.0035	-0.0027	0.0008	0.7714
AZN-9	C10-H10···O1	5	2.564	-0.0074	0.0074	0.0243	0.0052	-0,0042	0.0009	0.8077
	C14-H14B···N1	1	2.675	-0.0068	0.0068	0.0207	0.0043	-0.0035	0.0008	0.8140
	C17-H17A···Cg1	6	2.811	-0.0045	0.0045	0.0173	0.0036	-0.0028	0.0007	0.7778
	Cg1···Cg2	2	3.843	-0.0064	0.0064	0.0172	0.0036	-0.0028	0.0007	0.7778
		3		-0.0051	0.0051	0.0135	0.0028	-0.0022	0.0006	0.7857
	Cg2···Cg2	4	3.768	-0.0053	0.0053	0.0129	0.0027	-0.0022	0.0005	0.8148
AZN-10	C14-H14B···N1	1	2.714	-0.0064	0.0064	0.0200	0.0040	-0.0033	0.0007	0.8250
	Cg1···Cg2	2	3.768	-0.0061	0.0061	0.0163	0.0034	-0.0027	0.0007	0.7941
		3		-0.0062	0.0062	0.0171	0.0035	-0.0027	0.0008	0.7714
	Cg1···Cg2	4	3.643	-0.0064	0.0064	0.0180	0.0036	-0.0028	0.0008	0.7778
		5		-0.0062	0.0062	0.0171	0.0035	-0.0027	0.0008	0.7714
AZN-11	C24-H24A···N1	1	2.737	-0.0063	0.0063	0.0179	0.00378	-0.0030	0.0007	0.7937
	Cg1···Cg2	2	3.728	-0.0064	0.0064	0.0183	0.0037	-0.0028	0.0009	0.7568
		3		-0.0064	0.0064	0.0179	0.0036	-0.0028	0.0008	0.7778
	Cg1···Cg2	4	3.643	-0.0061	0.0061	0.0163	0.0034	-0.0027	0.0007	0.7941
		5		-0.0060	0.0060	0.0163	0.0034	-0.0026	0.0007	0.7647

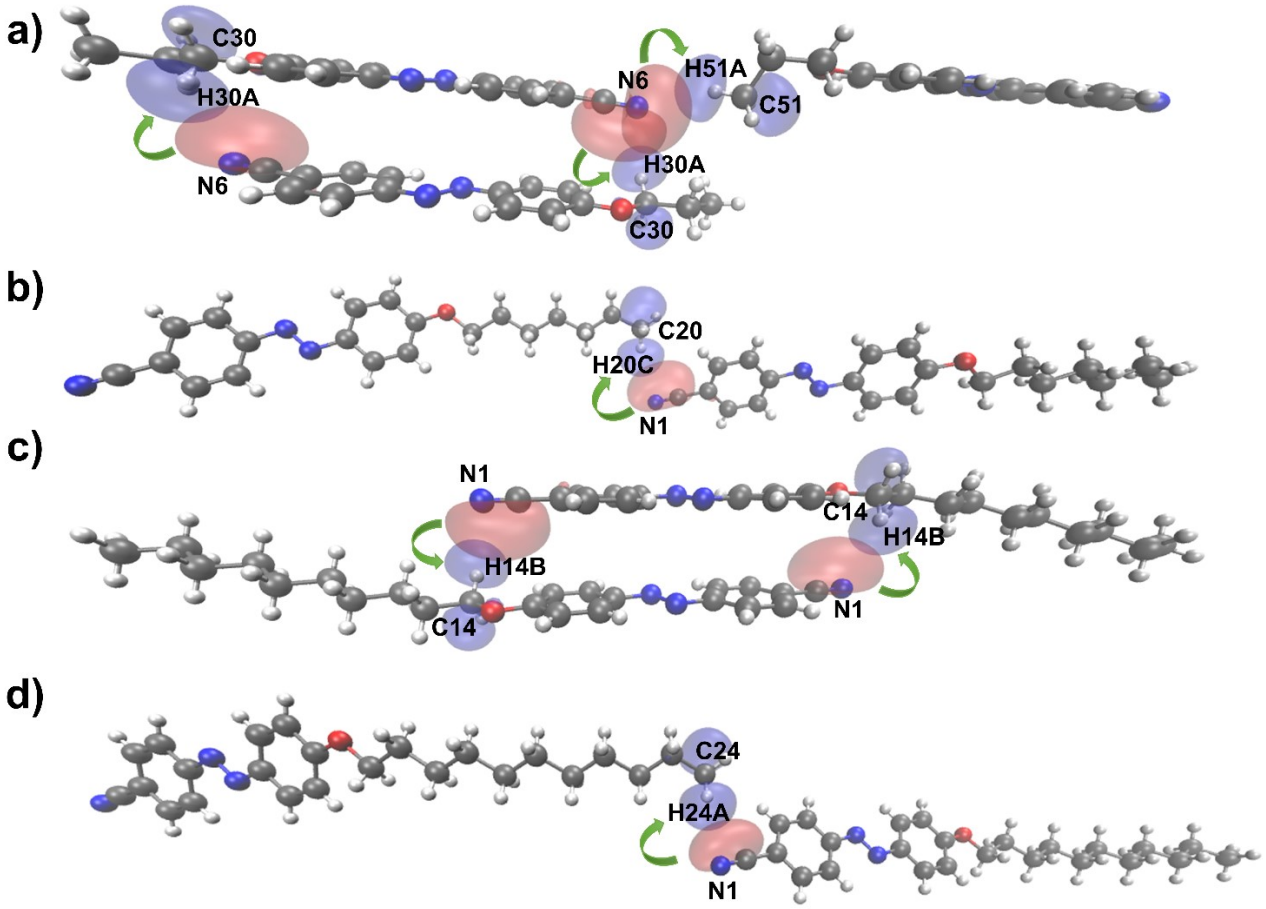

Fig. S24. NBO of C-H···N weak contacts for the crystal packing of the compounds, a) **AZN-3**, b) **AZN-7**, c) **AZN-10** and d) **AZN-11** showing the electron transfer.

Table S7. Second-order perturbated stabilization energy (E^2) along with NBOs participating in HBs.

Sample code	Donor NBO	Acceptor NBO	E^2 (kcal/mol)
AZN-3	C29 ≡ N6 (π)	C30-H30A (σ*)	0.07
	N6 (LP)	C51-H51A (σ*)	0.27
AZN-6	C1 ≡ N1 (π)	C14-H14B (σ*)	0.12
AZN-7	C1 ≡ N1 (π)	C20-H20C (σ*)	0.17
AZN-9	C1 ≡ N1 (π)	C14-H14B (σ*)	0.11
	Cg1 (π)	C17-H17A (σ*)	0.07
	O1 (LP)	C10-H10 (σ*)	0.33
AZN-10	C1 ≡ N1 (π)	C14-H14B (σ*)	0.12
AZN-11	C1 ≡ N1 (π)	C24-H24A (σ*)	0.22

Table S8. Phase transition table for the compounds, **AZN-n** (**n = 3 - 12**).

Compound code	Phase Transition Temperatures Heating /Cooling Cycle
AZN-3	Cry-Iso (137 °C) Iso-N (120 °C)-Cry (110 °C)
AZN-4	*Cry-N (126 °C)-Iso (132 °C) Iso-N (120 °C)-Cry (97 °C)
AZN-5	Cry- N (106 °C)-Iso (114 °C) Iso-N (113 °C)-Cry (87 °C)
AZN-6	Cry-N (100 °C)-Iso (115 °C) Iso-N (114 °C)-Cry (84 °C)
AZN-7	Cry-N (94 °C)-Iso (108 °C) Iso-N (107 °C)-Cry (73 °C)
AZN-8	*Cry-N (111 °C)-Iso (118 °C) Iso-N (106 °C)-Cry (72 °C)
AZN-9	Cry-Iso (105 °C) Iso-N (103 °C)-SmA (82 °C)-Cry (75 °C)
AZN-10	*Cry-N (111 °C)-Iso (112 °C) Iso-N (102 °C)-SmA (92 °C)-Cry (71 °C)
AZN-11	Cry-SmA (97 °C)- N (99 °C)-Iso (102 °C) Iso-N (101 °C)-SmA (98 °C)-Cry (75 °C)
AZN-12	Cry-Iso (105 °C) Iso-SmA (100 °C)-Cry (79 °C)

The data (*) is only obtained from hot stage POM analysis, Cry- Crystalline state, N- Nematic, SmA-Smectic A, Iso-Isotropic phase.

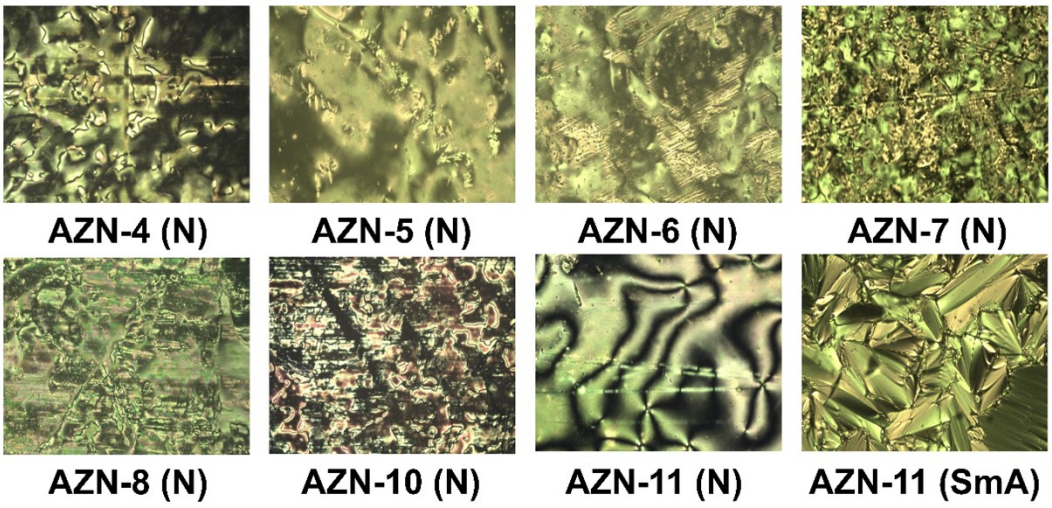

Fig. S25. Textures of liquid crystal phases by hot stage POM during heating cycle for **AZN-4** (N-126 °C), **AZN-5** (N-106 °C), **AZN-6** (N-100 °C), **AZN-7** (N-94 °C), **AZN-8** (N-111 °C), **AZN-10** (N-111 °C) and **AZN-11** (N-99 °C, SmA-97 °C) at 200X magnification.

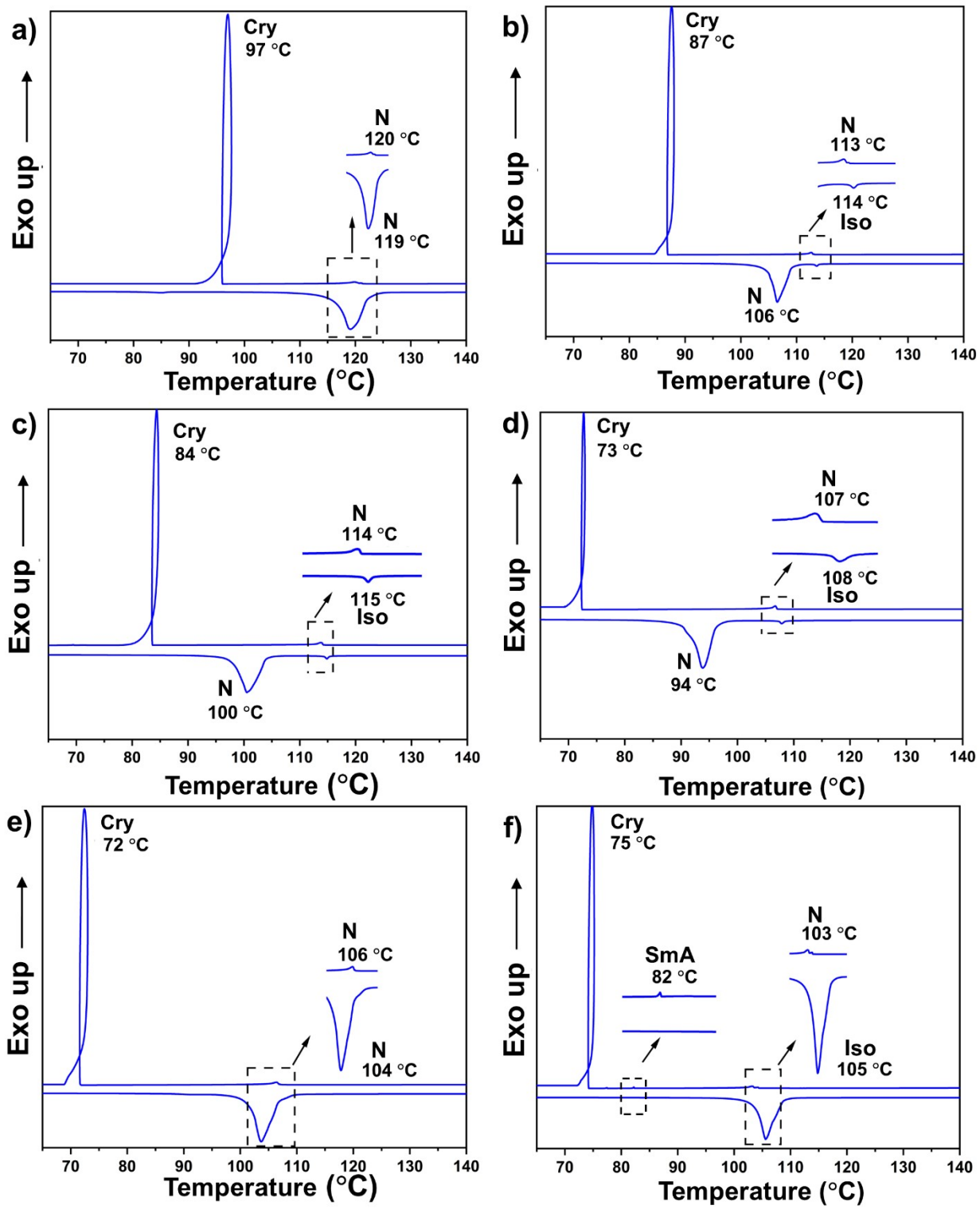

Fig. S26. DSC thermogram of a) **AZN-4**, b) **AZN-5**, c) **AZN-6**, d) **AZN-7**, e) **AZN-8** and f) **AZN-9.**

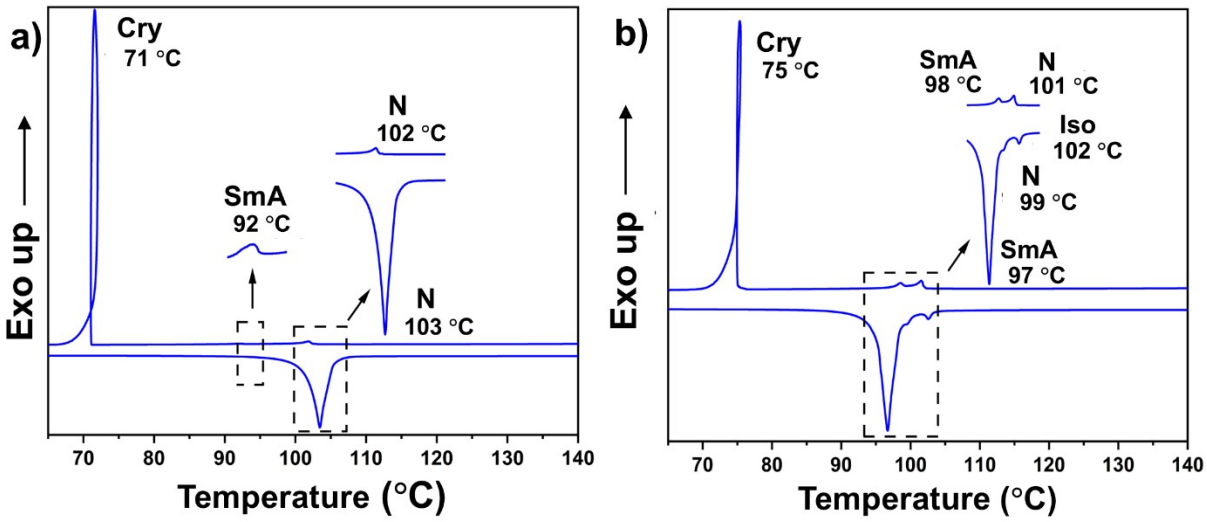

Fig. S27. DSC thermogram of a) **AZN-10** and b) **AZN-11.**

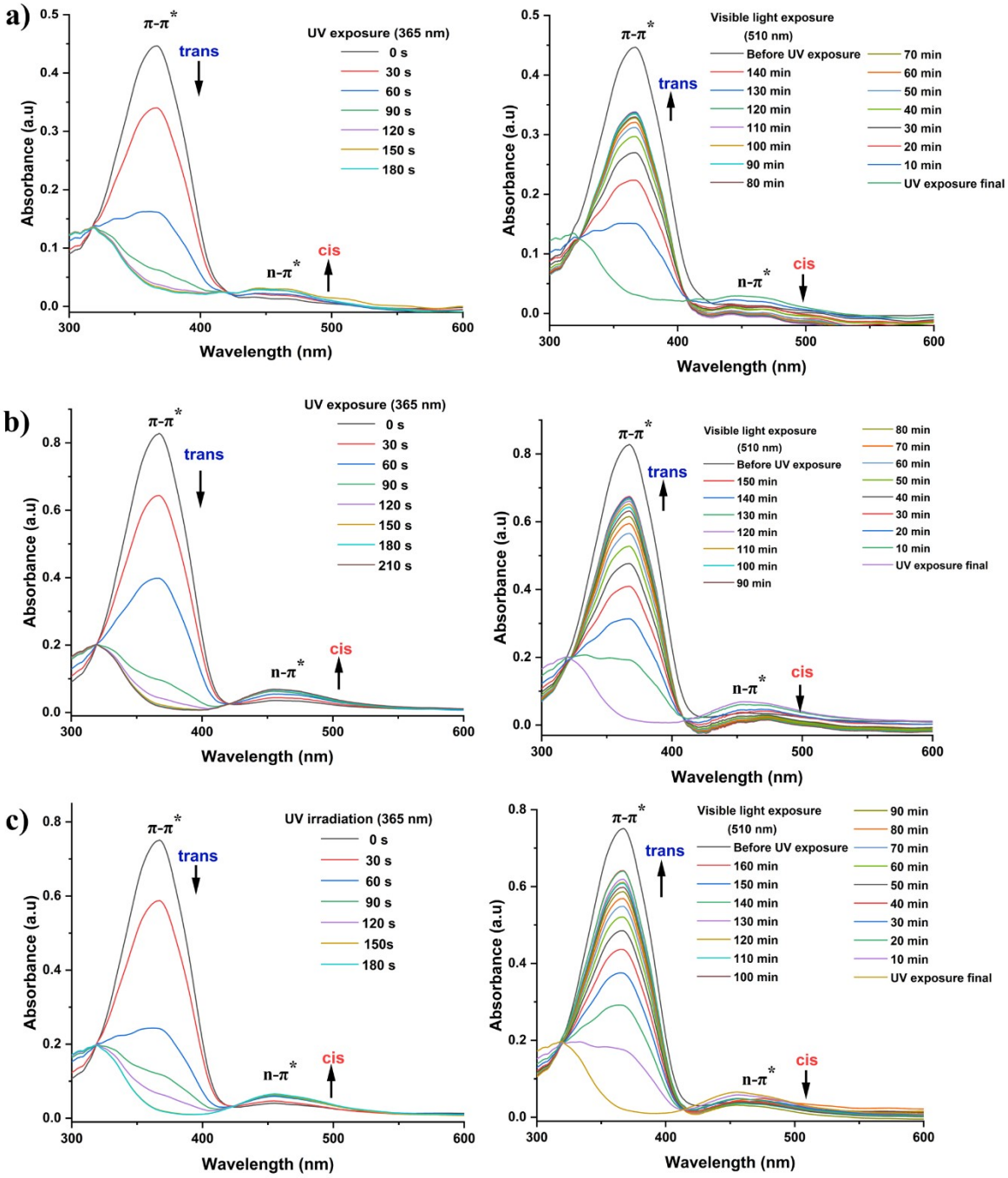

Fig. S28. Reversible isomerization between $E \rightarrow Z$ (left), $Z \rightarrow E$ (right) for a) **AZN-4**, b) **AZN-5** and c) **AZN-6**.

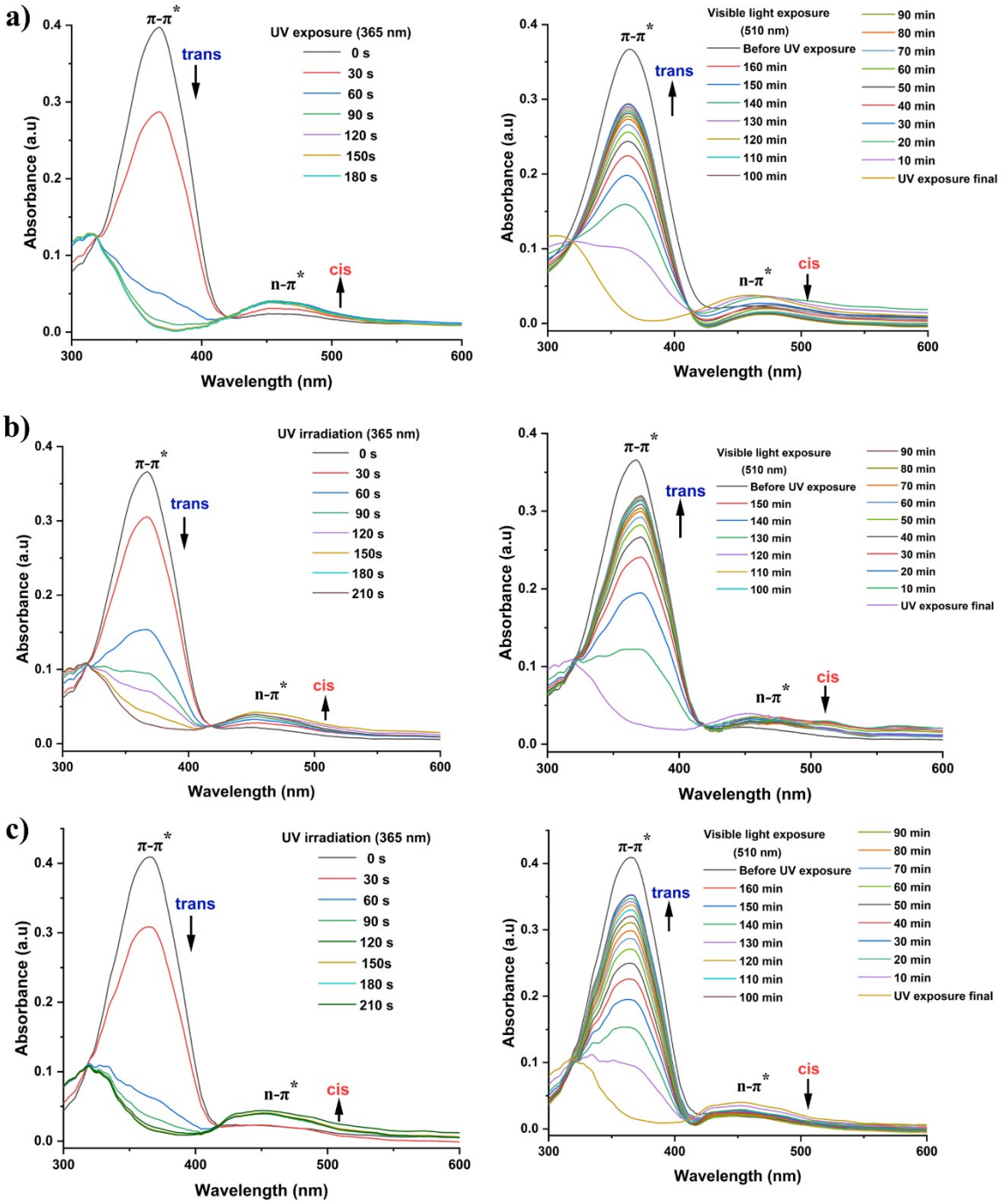

Fig. S29. Reversible isomerization between $E \rightarrow Z$ (left), $Z \rightarrow E$ (right) for $E \rightarrow Z$ (left), $Z \rightarrow E$ (right) a) **AZN-7**, b) **AZN-8** and c) **AZN-9**.

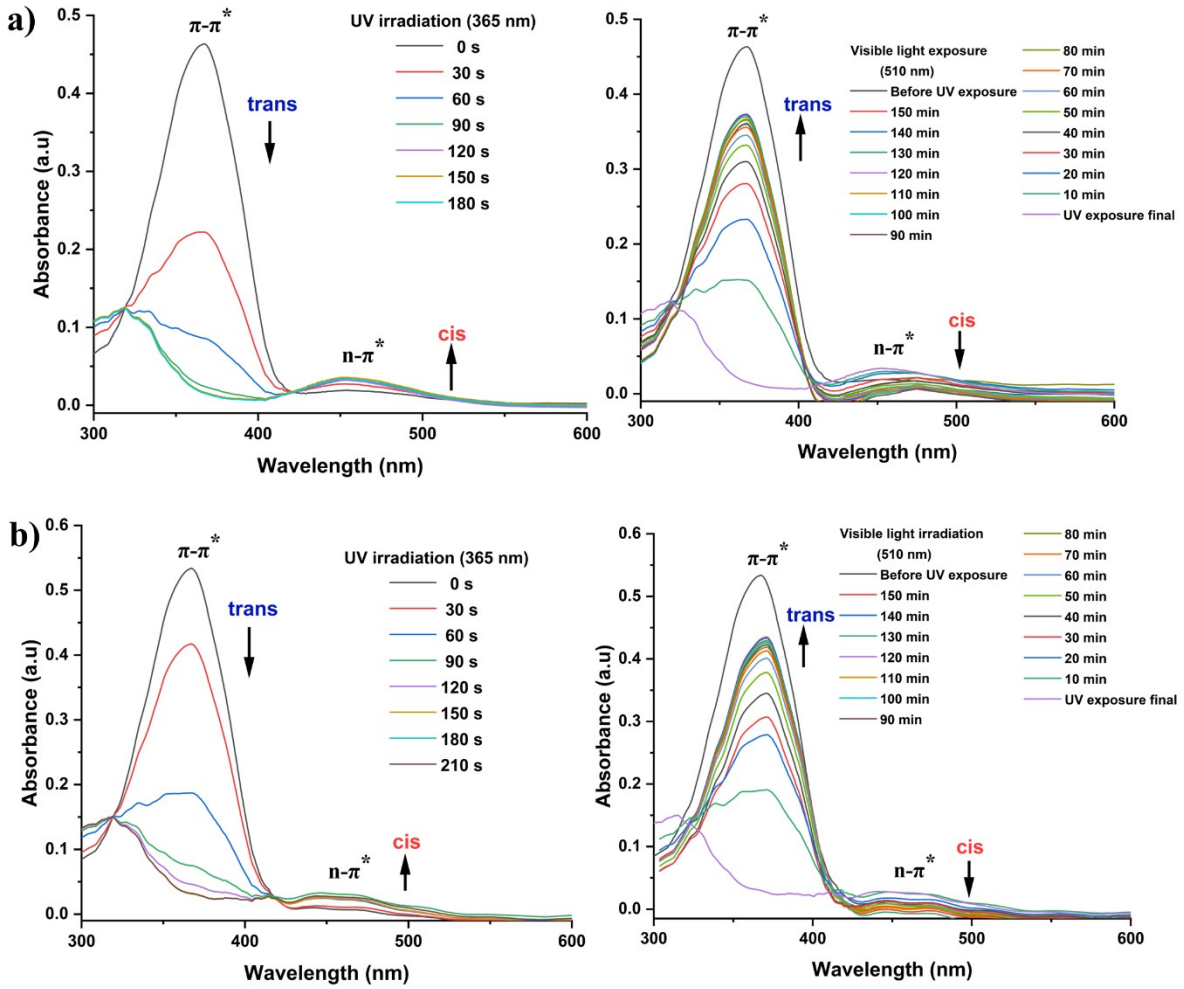

Fig. S30. Reversible isomerization between $E \rightarrow Z$ (left), $Z \rightarrow E$ (right) for a) **AZN-10** and b) **AZN-11**.

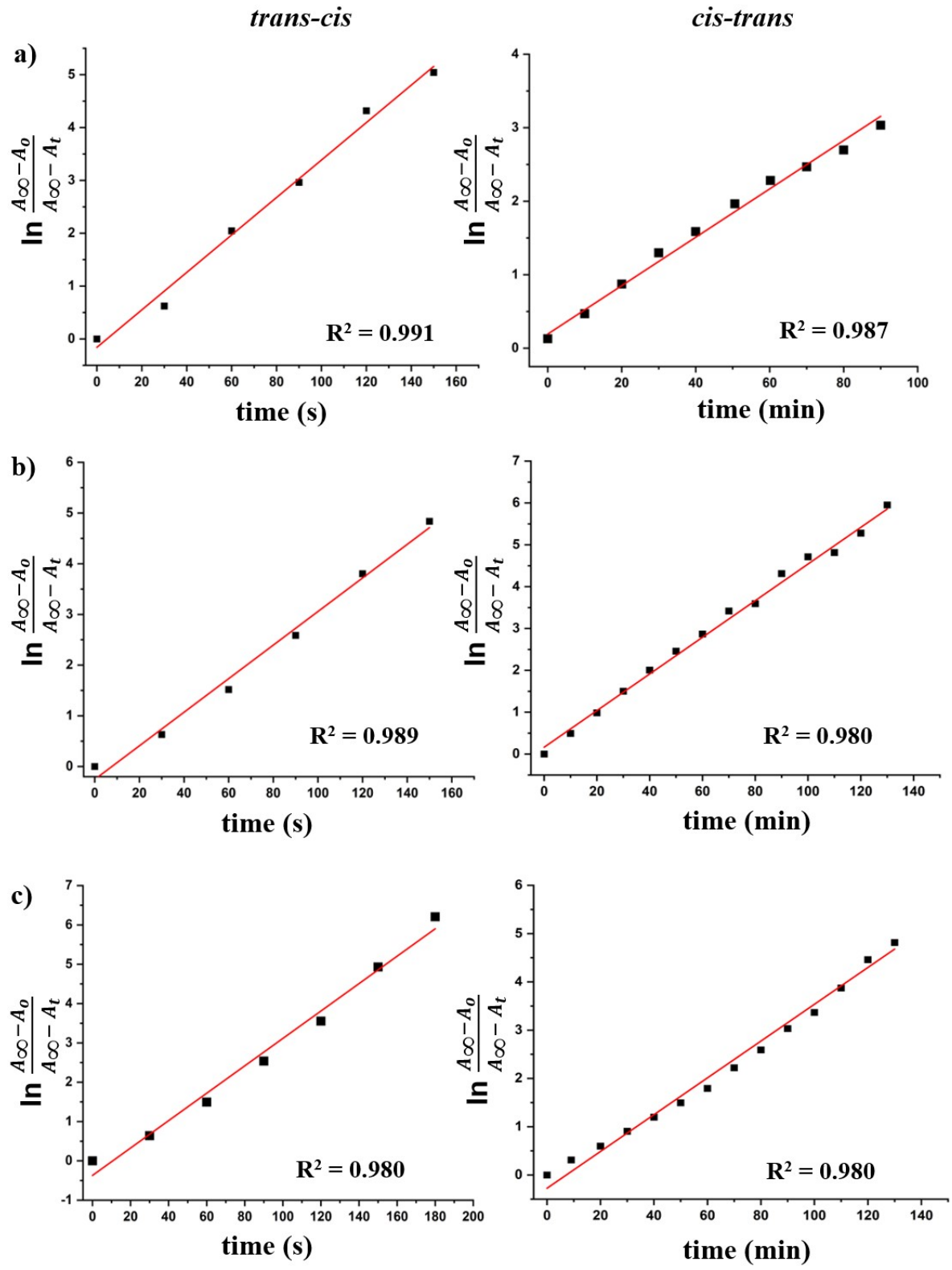

Fig. S31. Linear fit for the first-order kinetics of $E \rightarrow Z$ (left) and $Z \rightarrow E$ (right) isomerization for a) **AZN-3**, b) **AZN-4** and c) **AZN-5**.

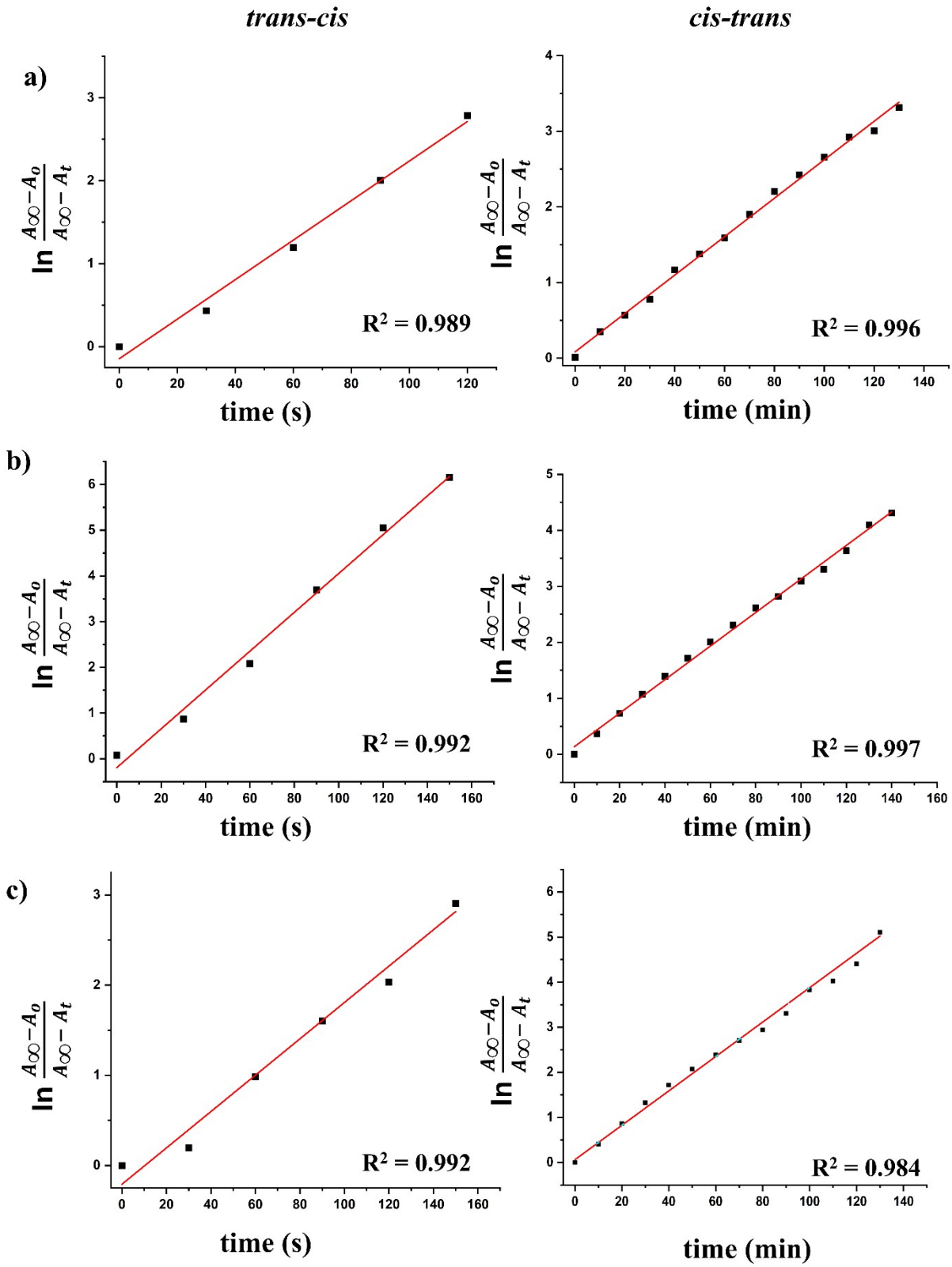

Fig. S32. Linear fit for the first-order kinetics of $E \rightarrow Z$ (left) and $Z \rightarrow E$ (right) isomerization for a) **AZN-6**, b) **AZN-7** and c) **AZN-8**.

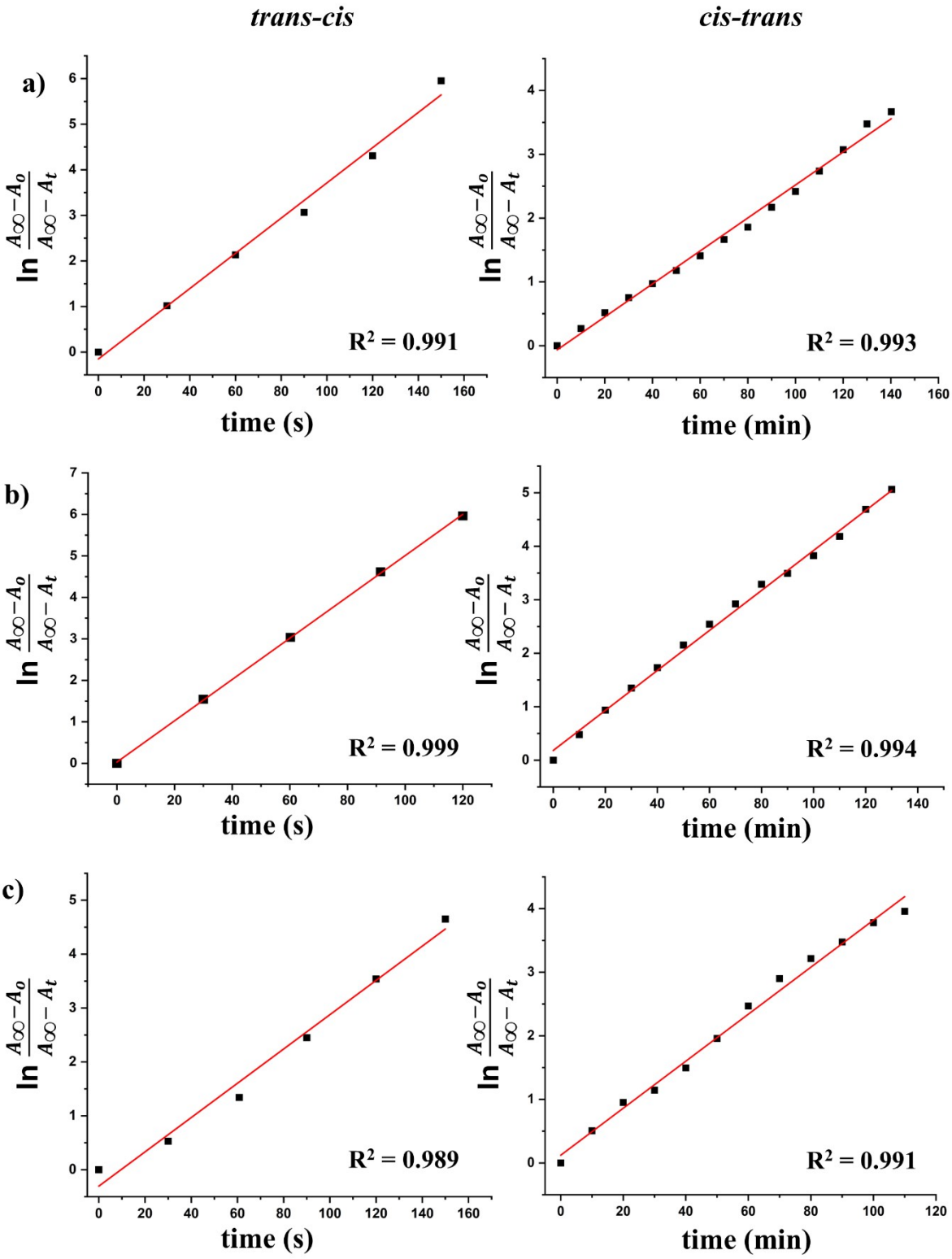

Fig. S33. Linear fit for the first-order kinetics of $E \rightarrow Z$ (left) and $Z \rightarrow E$ (right) isomerization for a) **AZN-9**, b) **AZN-10** and c) **AZN-11**.

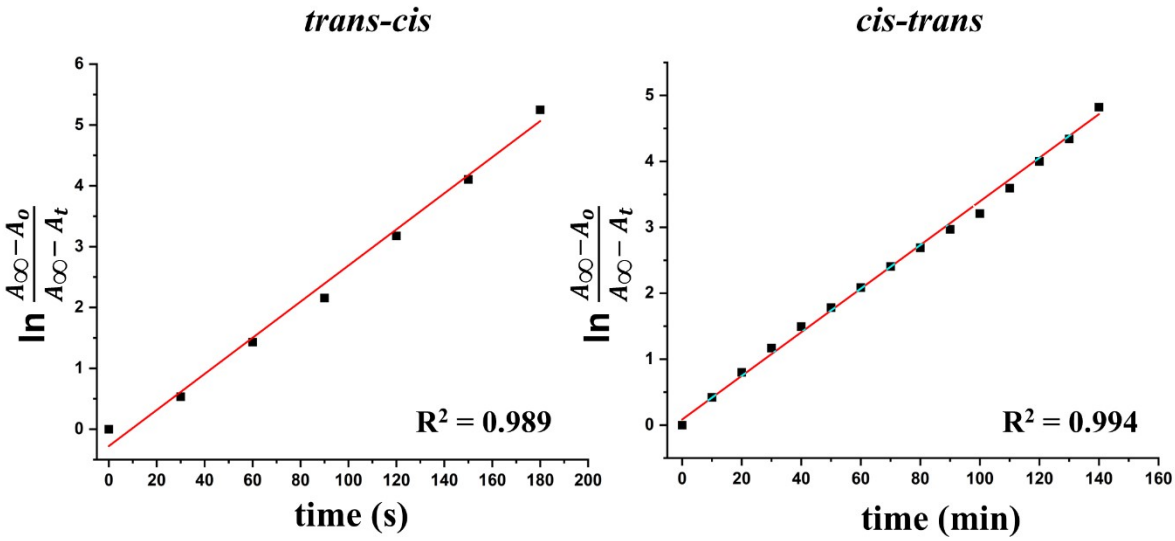

Fig. S34. Linear fit for the first-order kinetics of $E \rightarrow Z$ (left) and $Z \rightarrow E$ (right) isomerization for **AZN-12**.

Table S9. Percentage conversion efficiency ($E \rightarrow Z$) and kinetics of reversible $E \leftrightarrow Z$ isomerization for **AZN-n**.

Sample code	$E \rightarrow Z$			$Z \rightarrow E$		
	Conversion efficiency (%)	Rate constant (10^{-2} s^{-1})	PSS (sec)	Rate constant (10^{-2} min^{-1})	Half lifetime (min)	PSS (min)
AZN-3	94.4	3.545	120	3.205	21.6	140
AZN-4	93.1	3.595	150	4.378	15.8	120
AZN-5	97.8	3.694	150	3.811	18.2	130
AZN-6	97.2	2.443	150	2.539	27.3	140
AZN-7	98.5	4.046	120	2.997	23.3	140
AZN-8	93.2	2.016	180	3.817	18.1	130
AZN-9	96.1	3.864	150	2.655	26.1	150
AZN-10	96.6	4.975	120	3.740	18.5	130
AZN-11	94.1	3.272	150	3.697	18.8	140
AZN-12	95.1	3.041	150	3.308	22.5	130

References

1. A. Lausi, M. Polentarutti, S. Onesti, J. R. Plaisier, E. Busetto, G. Bais, L. Barba, A. Cassetta, G. Campi and D. Lamba, *Eur. Phys. J. Plus*, 2015, **130**, 1-8.
2. W. Kabsch, *Acta Crystallogr., Sect. D:Biol. Crystallogr.*, 2010, **66**, 125-132.
3. G. M. Sheldrick, *Sadabs*, 1996.
4. O. V. Dolomanov, L. J. Bourhis, R. J. Gildea, J. A. K. Howard and H. Puschmann, *J. Appl. Crystallogr.*, 2009, **42**, 339-341.
5. G. M. Sheldrick, *Acta Crystallogr., Sect. C:Struct. Chem.*, 2015, **71**, 3-8.
6. C. F. Macrae, I. J. Bruno, J. A. Chisholm, P. R. Edgington, P. McCabe, E. Pidcock, L. Rodriguez-Monge, R. Taylor, J. V. D. Streek and P. A. Wood, *J. Appl. Crystallogr.*, 2008, **41**, 466-470.
7. P. R. Spackman, M. J. Turner, J. J. McKinnon, S. K. Wolff, D. J. Grimwood, D. Jayatilaka and M. A. Spackman, *J. Appl. Crystallogr.*, 2021, **54**, 1006-1011.
8. M. A. Spackman and D. Jayatilaka, *CrystEngComm*, 2009, **11**, 19-32.
9. M. J. Turner, S. Grabowsky, D. Jayatilaka and M. A. Spackman, *J. Phys. Chem. Lett.*, 2014, **5**, 4249-4255.
10. A. Frisch, *Wallingford, USA, 25p*, 2009, **470**.
11. R. Dennington, T. A. Keith and J. M. Millam, *Semichem Inc.: Shawnee Mission, KS, USA*, 2016, 143-150.
12. T. Lu and F. Chen, *J. Comput. Chem.*, 2012, **33**, 580-592.
13. E. D. Glendening, C. R. Landis and F. Weinhold, *J. Comput. Chem.*, 2013, **34**, 1429-1437.
14. W. Humphrey, A. Dalke and K. Schulten, *J. Mol. Graphics*, 1996, **14**, 33-38.
15. O. Dash, J. S. Thakur, P. K. Mondal, M. Polentarutti and S. K. Nayak, *J. Mol. Liq.*, 2025, **433**, 127893.